

Reelin-Immunoreactive Neurons, Axons, and Neuropil in the Adult Ferret Brain: Evidence for Axonal Secretion of Reelin in Long Axonal Pathways

VERÓNICA MARTÍNEZ-CERDEÑO, MARÍA J. GALAZO, AND FRANCISCO CLASCÁ*
Neurodevelopment Laboratory, Department of Morphology, Autonomía University
School of Medicine, E-28029 Madrid, Spain

ABSTRACT

Reelin is a large secretable protein which, when developmentally defective, causes the *reeler* brain malformation in mice and a recessive form of lissencephaly with cerebellar hypoplasia in humans. In addition, Reelin is heavily expressed throughout the adult brain, although its function/s there are still poorly understood. To gain insight into which adult neuronal circuits may be under the influence of Reelin, we systematically mapped Reelin-immunoreactive neuronal somata, axons, and neuropil in the brain and brainstem of ferrets. Results show that Reelin immunoreactivity is found in widespread but specific sets of neuronal bodies, axonal tracts, and gray matter neuropil regions. Depending on the region, the immunoreactive neuronal somata correspond to interneurons, projection neurons, or both. Some well-defined axonal projection systems are immunoreactive, whereas most other white matter tracts are unlabeled. The labeled pathways include, among others, the lateral olfactory tract, the entorhinohippocampal (perforant) pathway, the retroflex bundle, and the stria terminalis. Labeled axons in these tracts contain large numbers of discrete, very small, immunoreactive particles, suggestive of secretory vesicles under the light microscope. The neuropil in the terminal arborization fields of these axons is also heavily immunoreactive. Taken together, our observations are consistent with the notion that some neurons may anterogradely transport Reelin along their axons in large membrane-bound secretory vesicles (Derer et al. [2001] *J. Comp. Neurol.* 440:136–143) and secrete it into their terminal arborization fields, which may be quite distant from the somata synthesizing the protein. These findings have implications for identifying where Reelin acts in adult brain circuits. *J. Comp. Neurol.* 463:92–116, 2003. © 2003 Wiley-Liss, Inc.

Indexing terms: cerebral cortex; olfactory bulb; hippocampus; cerebellum; thalamus; synaptic plasticity

Reelin was identified in 1995 (D'Arcangelo et al., 1995) as the defective protein in the widely studied mutant mice strain *reeler* (Falconer, 1951, Caviness et al., 1988). The Reelin gene is also mutated in a recessive form of human lissencephaly with cerebellar hypoplasia (Hong et al., 2000). A large, secretable protein (Miyata et al., 1996; D'Arcangelo et al., 1997; Lacor et al., 2000; Jossin and Goffinet, 2001), Reelin is present in specific neuronal populations of the central nervous system (D'Arcangelo et al., 1995, 1997; Miyata et al., 1996; Schiffmann et al., 1997; Alcántara et al., 1998; Drakew et al., 1998; Pesold et al., 1998, 1999; Impagnatiello et al., 1998; Rodríguez et al., 2000; Guidotti et al., 2000; Zecevic and Rakic, 2001; Martínez-Cerdeño et al., 2002), as well as in several other body tissues (Smalheiser et al., 2000; Hong et al., 2000; Heymann et al., 2001). There is evidence indicating that Reelin may regulate cell adhesion, acting either as a se-

creted intercellular signaling molecule between neurons (reviewed by Rice and Curran, 2001) or as a secreted protease of the extracellular matrix (Quattrocchi et al.,

Grant sponsor: Fondo de Investigación Sanitaria; Grant number: 98/0286; Grant number: BEFI 99/9160; Grant sponsor: Ministerio de Educación y Cultura; Grant number: PB 97/015; Grant sponsor: Ministerio de Ciencia y Tecnología; Grant number: BMC2001-0623; Grant sponsor: the Eugenio Rodríguez Pascual Foundation (Spain).

*Correspondence to: Francisco Clascá, Neurodevelopment Laboratory, Department of Morphology, Autónoma University School of Medicine, Ave. Arzobispo Morcillo s/n., E-28029 Madrid, Spain.
E-mail: francisco.clasca@uam.es

Received 25 September 2002; Revised 19 December 2002; Accepted 20 February 2003

DOI 10.1002/cne.10748

Published online the week of June 23, 2003 in Wiley InterScience (www.interscience.wiley.com).

2002). During development, Reelin is believed to regulate the cell-to-cell interactions that lead to the correct positioning of some neuroblast populations at the end of their migration (Rice and Curran, 2001; Olson and Walsh, 2002) and, accordingly, the *reeler* brain phenotype is characterized by widespread cytoarchitectural anomalies (reviewed in Caviness et al., 1988; see also Phelps et al., 2002).

Intriguingly, Reelin has been found to be heavily and widely expressed in the adult brain (Alcántara et al., 1998; Pesold et al., 1998; Drakew et al., 1998; Impagnatiello et al. 1998, Rodríguez et al., 2000, 2002; Guidotti et al., 2000; Pérez-García et al., 2001; Zecevic and Rakic, 2001; Martínez-Cerdeño and Clascá 2002; Haas et al., 2002; Martínez-Cerdeño et al., 2002), but its functional role in adult neurons is as yet unknown. It has been suggested

Abbreviations

5M	motor trigeminal nucleus	MAN	medial amygdaloid nucleus
5P	principal trigeminal nucleus	MCL	mitral cell layer of the olfactory bulb
A	lamina A of the dorsal lateral geniculate nucleus	MEA	medial entorhinal area
A1	lamina A1 of the dorsal lateral geniculate nucleus	Me5	mesencephalic trigeminal tract
AAA	anterior amygdaloid area	ML	molecular layer
ABAN	accessory basal amygdaloid nucleus	Mm	mammillary bodies
AC	anterior commissure	MPo	medial preoptic area
Acb	nucleus accumbens	MRN	medial reticular nucleus
AIC	agranular insular cortex	MSP	medial septal nucleus
AM	anteromedial thalamic nucleus	NLOT	nucleus of the lateral olfactory tract
AnB	angular bundle	OGL	granule cell layer of the olfactory bulb
AOB	accessory olfactory bulb	OPL	optic nerve layer of the superior colliculus.
AON	anterior olfactory nucleus	OpT	optic tract
AOTN	nucleus of the accessory optic tract	Or	stratum oriens
Av	alveus	OT	olfactory tuberculum
AVCN	anteroventral cochlear nucleus	PaS	parasubiculum
BAN	basal amygdaloid nucleus	PBD	dorsal parabrachial nucleus
BC	brachium conjunctivum	PBM	medial parabrachial nucleus
CGL	granular cell layer of the cerebellar cortex	PCL	Purkinje cell layer
C	lamina C of the dorsal lateral geniculate thalamic nucleus	PCN	posterior commissure nucleus
CA1	Ammon's Horn sector 1	PG	periaqueductal gray matter
CA3	Ammon's Horn sector 3	PHA	posterior hypothalamic area
CA4	Ammon's Horn sector 4	PL	plexiform layer
Cd	caudate nucleus	PN	pontine nuclei
CoAN	cortical amygdaloid nucleus	Po	posterior thalamic nucleus
CoAT	corticoamygdaloid transitional area	PrC	perirhinal cortex
CS	corticospinal tract (longitudinal pontine fibers)	PrS	prosubiculum
CSR	centralis superior raphe nucleus	PT	parataenial thalamic nucleus
DB	diagonal band nuclei	PTN	pretectal nuclei
DCN	dorsal cochlear nucleus	Pu	putamen
DG	dentate gyrus	Pul	pulvinar nucleus
dLGN	dorsal lateral geniculate nucleus	Pv	periventricular white matter of the olfactory bulb.
DLEA	dorsolateral entorhinal area	PVCN	posteroventral cochlear nucleus
DRN	dorsalis raphe nucleus	PVH	paraventricular hypothalamic nucleus
DS	deep stratum of the superior colliculus	PyC	pyriform cortex
EN	endopyriform nucleus	Pyr	pyramidal stratum of Ammon's Horn
EPL	external plexiform layer of the olfactory bulb	Rd	stratum radiatum
EpN	entopeduncular nucleus	Re	reuniens thalami nucleus
Fx	retrocommissural fornix	ReIn-ir	reelin-immunoreactive
GCL	granule cell domains of the cochlear nucleus	RN	raphe nuclei
GLL	glomerular layer of the olfactory bulb	RTN	reticular thalamic nucleus
Gn	granule cell layer of the dentate gyrus	Sb	subiculum
GrL	granule cell layer of the olfactory bulb	SC	superior colliculus
Hb	habenula	SGS	superficial gray stratum of the superior colliculus
HF	hippocampal fissure	SI	substantia innominata
I	layer I of the cerebral cortex; Ia or Ib indicate the superficial and deep sublayers, respectively (see text).	Sm	submedial thalamic nucleus
ICj	islands of Calleja	SNR	substantia nigra pars reticulata
IGS	intermediate gray stratum of the superior colliculus	SON	superior olivary nucleus
II	layer II of the cerebral cortex; IIa or Ib indicate superficial and deep sublayers, respectively	STh	subthalamic nucleus
III	layer III of the cerebral cortex	SV	spinal trigeminal nucleus
IV	layer IV of the cerebral cortex	SZ	stratum zonale of the superior colliculus
IPL	internal plexiform layer of the olfactory bulb	TT	tenia tecta
ISp	intermediate septal nucleus.	V	layer V of the cerebral cortex
IpN	interpeduncular nucleus	VA-VL	ventralis anterior-ventralis lateralis thalamic complex
LAN	lateral amygdaloid nucleus	VI	layer VI of the cerebral cortex
LD	lamina dissecans of the entorhinal cortex	7N	seventh cranial nerve (facial nerve)
LEA	lateral entorhinal area	8N	eight cranial nerve (vestibulocochlear nerve)
LHA	lateral hypothalamic area	Vm	ventralis medialis thalamic nucleus
LM	stratum lacunosum moleculare	VMH	ventromedial hypothalamic nucleus
LOT	lateral olfactory tract	VN	vestibular nuclei
LP	lateral posterior thalamic nucleus	VP	ventral pallidum
LPo	lateral preoptic area	WIS	intermediate white stratum of the superior colliculus
LSp	lateral septal nucleus	WM	subcortical white matter
		XII	hypoglossal nucleus
		ZI	zona incerta

that, acting either as an intercellular signaling molecule (Pesold et al., 1999; Rodríguez et al., 2000), as an extracellular matter protease (Quattrocchi et al., 2002), or as both, Reelin might modulate synaptic plasticity in specific brain circuits. Precise identification of the brain circuits containing Reelin, therefore, could provide important clues on both Reelin function/s and the neuronal circuits under its influence. However, Reelin protein-mapping data in adult mammals (Miyata et al., 1996; Pesold et al., 1998; Impagnatiello et al., 1998; Guidotti et al., 2000; Rodríguez et al., 2000; Zecevic and Rakic, 2001; Pérez-García et al., 2001; Martínez-Cerdeño and Clascá, 2002) have focused on the cerebral and cerebellar cortices, to the point that the available information about other brain regions consists only of some fragmentary data in rodents (Pesold et al., 1998) and a recent study from our laboratory in macaques (Martínez-Cerdeño et al., 2002). Moreover, although the putative modulatory function of Reelin in synaptic plasticity is likely to take place mainly in the gray matter neuropil, information on neuropil distribution of Reelin is very limited (Pesold et al., 1998; Pappas et al., 2002; Martínez-Cerdeño et al., 2002).

To obtain a comprehensive view of the neuronal circuits that may be under the influence of Reelin in adult carnivores, we conducted a light-microscope analysis of Reelin immunoreactivity in the brain and brainstem of adult ferrets. For our study, we chose the ferret (*Mustela putorius*) because, despite being a widely used model species for studies of brain development and plasticity, available data on Reelin distribution in ferrets, or any other carnivore mammals, are very limited (Noctor et al., 1999; Pérez-García et al., 2001, Martínez-Cerdeño and Clascá, 2002). Moreover, in a parallel study (Martínez-Cerdeño et al., 2000), we had already begun investigating the developmental sequence of Reelin expression in embryonic and postnatal ferrets.

Results show that Reelin immunoreactivity is widely distributed in specific sets of neuronal bodies, axonal tracts, and gray matter neuropil areas. Our light-microscope findings are consistent with the notion that several populations of projection neurons transport large amounts of Reelin along their axons in secretory vesicle-like particulate structures and secrete the protein at their terminal arborization fields. Thus, in the adult, Reelin may exert its effect in the neuropil of brain regions that are quite distant from the somata of the neurons that synthesize the protein.

MATERIALS AND METHODS

Brain tissue from four adult pigmented female ferrets (*Mustela putorius furo*) was used for the present study. Animals were obtained from a commercial breeder (Marshall Farms Europe). Procedures involving these animals were carried out in accordance with the European Community's Council Directive 86/609/EEC, and NIH guidelines, and approved by our University's Bioethics Committee. Animals were killed with sodium pentobarbital (80 mg/kg i.p.).

Pilot experiments with the antibodies we intended to use in this study yielded widely variable results between experiments. We, therefore, tested several perfusion protocols and a variety of tissue pretreatments and antibody concentrations; the best labeling results were obtained with the protocol that is described below.

Immediately after killing, animals were perfused through the left ventricle with saline (5 minutes), followed by cold (4°C) 4% paraformaldehyde in 0.1 M phosphate buffer pH 7.4 (PB) for 30 minutes. Once perfusion was completed, brains were stereotaxically split into two coronal blocks and removed from the skull. Brains were then post-fixed by immersion in the same fixative for 24 hours at 4°C. Tissue blocks were cryoprotected by soaking in sucrose solutions of ascending concentration (10–30%) in PB until they sank. Series of 40- μ m-thick coronal sections were then obtained on a freezing microtome. For cytoarchitectonic reference, one series of sections was mounted onto gelatin-coated glass slides, air-dried, stained with cresyl violet, dehydrated, and cover-slipped. The remaining series were either immediately processed for immunohistochemistry, or soaked in a 20% glycerol solution in PB (2 hours), and stored at –20°C in this solution.

Immunohistochemistry

From each brain, we selected a sample of 10–15 coronal sections covering a variety of rostrocaudal levels of the olfactory bulbs, cerebral hemispheres, diencephalon, rostral brainstem, and cerebellum. Before beginning the immunohistochemical protocol, sections that had been preserved in glycerol were thoroughly rinsed in PB at 4°C for 48 hours.

Free-floating sections were first rinsed with a 1% hydrogen peroxide solution in phosphate-buffered saline (PBS) solution for 20 minutes to bleach out endogenous peroxidase activity. As a pretreatment for retrieving epitopes blocked by paraformaldehyde, the sections were then soaked in citrate buffer pH 6.0, microwaved in this buffer at 700 W until boiling and left simmering in the buffer for 2 minutes, before being transferred to fresh citrate buffer at room temperature. Sections were then rinsed in PB and subsequently blocked with 10% horse serum + 3% bovine serum albumin + 1% Triton X-100 in 0.1 M PBS. Sections were incubated for 24 hours at room temperature either in mouse monoclonal immunoglobulin (Ig) G 142 (1:400, a gift of Dr. A.M. Goffinet, Namur, Belgium) or in mouse monoclonal IgG CR-50 (1:100, a gift of Dr. M. Ogawa, Riken, Japan). As secondary antibody, we used biotinylated horse anti-mouse IgG (Pierce, 1:200) for 90 minutes. Antibodies were diluted in 0.1 M PBS containing 3% normal horse serum and 0.3% Triton X-100. Sections were subsequently incubated in avidin-biotinylated horseradish peroxidase complex (ABC, Vector Laboratories) in 0.1 M PBS for 2 hours at room temperature and developed with 0.001% H₂O₂ + 0.04% 3,3'-diaminobenzidine tetrahydrochloride (DAB) in acetate buffer, pH 6. In most experiments, we included 1% nickel ammonium sulfate in the developing medium to enhance the opacity of the reaction product. Multiple rinses in PBS were performed between each of the above steps. The specificity of the monoclonal antibodies used is well characterized (De Bergueyck et al., 1998). In addition, we included primary antibody-free controls in each experiment, and these controls always evidenced an absence of immunostaining. Sections were mounted on gelatin-coated glass slides and air-dried. For a precise identification of the staining and nonstaining cell groups, some sections were lightly counterstained with thionin. Sections were finally dehydrated in graded alcohols, cleared in xylene, and cover-slipped with DePeX.

Selected sections were post-fixed in osmium tetroxide (2% in 0.1 M cacodylate buffer) after immunostaining. The sections were then dehydrated and flat-embedded in Araldite. Small (~2 mm²) tissue samples containing regions of interest were dissected from the sections. These samples were reincluded in Araldite and semithin sections (1–2 µm) were serially obtained on a Reichert Ultracut ultramicrotome. The semithin sections were counterstained with toluidine blue, mounted on glass slides, and dry-cover-slipped.

Imaging

Sections were examined in a Nikon Eclipse 400 microscope under bright- and darkfield illumination. Resolving the various patterns of immunolabeling required the systematic use of 1,000× oil-immersion optics for every investigated brain region. Tissue images were acquired with 4–100× planapochromatic objectives by using a SPOT camera (Diagnostic Instruments) with an initial 12-bit tone scale in a single focal plane; depth-of-field enhancing algorithms were not used. Canvas software (v.8, Deneba Systems) was used for digital processing and figure composition on an Apple G4 computer. Processing consisted of various combinations of adjustments in tone scale, gamma, and sharpness as needed to obtain optimal images. Local retouching was limited to areas outside the brain. In many cases, multiple images were assembled as montages in Canvas; borders between images were not retouched.

Cytoarchitectonic nomenclature

Although a growing body of literature is available on the ferret brain, cytoarchitectonic studies are not yet available for many of the brain regions labeled in our experiments. Thus, in addition to our own unpublished ferret data, identification of the various structures relied on published cytoarchitectonic studies of the cat brain (Berman, 1968; Avendaño and Reinoso-Suárez, 1975; Krettek and Price, 1977; Berman and Jones, 1982; Room and Groenewegen, 1986), which is structurally quite similar to the ferret brain. For the olfactory areas and their cortical layers, we followed the more precise nomenclature proposed by Price and coworkers in the rat (Price, 1973; Haberly and Price, 1978). Our use of terms to describe the shape (multipolar, fusiform, bipolar, globular, etc.) of immunolabeled neuronal somata follows the definitions recently proposed by Ekstrand and colleagues (2001).

RESULTS

General features of the labeling

Reelin-like immunoreactivity was localized into specific neuronal populations throughout the brain and brainstem. Immunostained structures included (1) some neuronal somata and frequently their proximal dendrites and axons, (2) some axonal tracts, and (3) areas of gray matter neuropil. No labeling was detected in glial, pial, or endothelial cells. Both of the two monoclonal anti-Reelin IgGs assayed in this study resulted in similar staining, although the CR-50 antibody yielded a weaker labeling and higher background. A comprehensive account of our observations is condensed in graphic form in Tables 1 and 2.

The number of the Reelin-immunoreactive (ReIn-ir) neuronal somata often varied widely between neighboring

TABLE 1. Reelin-Immunoreactive Neuronal Somata and Neuropil in Telencephalic Regions¹

	Neuronal somata	Neuropil/axons
<i>Olfactory bulb</i>		
Main olfactory bulb		
Glomerular layer (periglomerular cells)	○○○	+
Superficial plexiform layer (tufted cells)	●●○	++
Mitral cell layer	●●●	+
Inner plexiform layer	○	++
Granular layer	○	+
Lateral olfactory tract		+++
Accessory olfactory bulb	●●○	+
<i>Olfactory cortical areas</i>		
Anterior olfactory nucleus		
Molecular layer	●○	+++
Pyramidal layer	○	+
Multiform layer	●○	+
Endopyriform nucleus	●○	+
Olfactory tubercle	●	+++
Nucleus of the lateral olfactory tract	●	+
Prepyriform cortex		
Molecular layer	●	+++
Pyramidal layer	●●	+
Polymorph layer	●○	+
<i>Other basal telencephalic regions</i>		
Preoptic areas	●●○	++
Septo-hippocampal junction	●○	+
Diagonal band of Broca	●●○	+
Septal nuclei		
Medial	●●○	++
Lateral ventral	○○○	+
Other	○	+
Substantia innominata / anterior amigdaloid areas	●●○	++
Ventral pallidum	○	+
Bed nucleus of stria terminalis	○	+
Stria terminalis	●	+++
Globus pallidus	○	+
Striatum (caudate/putamen/accumbens)	○○○	+
Amygdaloid complex		
Corticomedial group	●●○	++
Basolateral group	●●	+
Central nuclei	○	+
Claustrum	●○	+
<i>Hippocampal formation and parahippocampal cortex</i>		
Fascia dentata		
Str. moleculare	●●○	+++
Str. granulare		
Hilus	●●○	+
Cornu Amonnis		
Str. lacunosum-moleculare	●●○	+++
Str. radiatum	●○	+
Str. pyramidale	○	
Str. oriens	●○	+
Alveus		
Subicular complex		
Str. moleculare	●●○	++
Str. pyramidale	●	+
Str. oriens	●	+
Entorhinal cortex		
Layer I	●●	+++
Layer II	●●○	+
Layer III	●○	+
Layer IV	●○	+
Layer V	●○	+
White matter (interstitial cells)	●	
<i>Isocortex</i>		
Layer I	●●○	+++
Layer II	●○○	+
Layer III	●○	+
Layer IV	●○	+
Layer V	●○	+
Layer VI	●○	+
White matter (interstitial cells)	●	

¹Localization and relative proportions of Reelin-immunoreactive neuronal somata and neuropil in olfactory, subcortical, and cortical telencephalic regions. For descriptive purposes, labeled neuronal somata are classified in two main categories: those containing heavy immunoprecipitate (filled circles) and those displaying weaker labeling (open circles). Circles represent a gross approximation of the relative number of each type of immunoreactive somata in a nucleus or layer (1 small circle, occasional isolated cells; 1 large circle, numerous cells; 2 large circles, all, or nearly all, the neurons are labeled). Likewise, crosses are used to represent differences in the density of neuropil/axonal immunoreactivity (+, faint labeling; ++, dense labeling; +++, very heavy labeling). Note that most of the brain regions contained some immunoreactive neuronal populations, and that some axonal pathways, such as the lateral olfactory tract and the stria terminalis, were heavily immunoreactive.

TABLE 2. Reelin-Immunoreactive Neuronal Somata and Neuropil in Diencephalic and Brainstem Regions¹

	Neuronal somata	Neuropil/axons
<i>Ventral thalamic structures</i>		
Zona incerta / Fields of Forel	●○	+
Reticular thalamic nucleus	○	+
Ventral lateral geniculate nucleus	○○	+
Entopeduncular nucleus	●●	+
Subthalamic nucleus	●●	+
<i>Hypothalamus</i>		
Paraventricular nucleus	●●●	++
Mammillary bodies	●	+
Other hypothalamic nuclei	●●	+
<i>Dorsal thalamus and epithalamus</i>		
Nuclei of dorsal thalamus	●○○	+
<i>Habenular nuclei</i>		
Medial	●●○	++
Lateral	●●●	++
Fasciculus retroflexus		+++
<i>Preteectum and mesencephalon</i>		
<i>Preteectal nuclei</i>		
Anterodorsal nucleus	●●●	+
Other preteectal nuclei	●○	+
<i>Superior colliculus</i>		
Stratum zonale	●○○	+++
Other layers	○○	+
<i>Inferior colliculus</i>		
Dorsal cortex	○○	+
Other subdivisions	○	+
Periaqueductal gray matter	○○	+
Terminal nuclei of the accessory optic system	●●○	++
<i>Substantia nigra</i>		
Pars compacta,	●○	+
Pars reticulata	○	+
Ventral tegmental area	○	+
Red nucleus	○	+
Interpeduncular nucleus	○	+++
<i>Pons cerebellum, medulla</i>		
Raphe nuclei	●○	+
Reticular nuclei	●○	+
Principal and motor trigeminal nuclei	●○	+
Spinal trigeminal nucleus	○	+
Pontine nuclei	●○○	+
Superior olivary complex	●○	+
Parabrachial nuclei	●○○	+
<i>Cochlear nuclei</i>		
Granule cell layer	○○○	+
Other cochlear nuclei	○	+
<i>Vestibular nuclei</i>		
Oculomotor, facial, abducens nuclei	○	+
Hypoglossal nucleus	●○	+
<i>Cerebellar cortex</i>		
Molecular layer	○	+++
Purkinje cell layer		+
Granular layer	○○○	+
White matter		
Deep cerebellar nuclei	○	+
Inferior olivary nucleus		+

¹Localization and relative proportion of Reelin-immunoreactive neuronal somata and neuropil in diencephalic and brainstem regions. Graphic conventions as in Table 1. Comparison with Table 1 shows that heavily immunoreactive neurons were, overall, scarcer in the brainstem than in the prosencephalic regions.

nuclei or cell layers. Moreover, thionin counterstaining of immunolabeled sections showed that the relative proportion of ReIn-ir cells to the total in the same layer or nucleus could also be quite variable (Tables 1, 2). The ReIn-ir somata displayed a wide range of staining intensities, from cells whose soma, proximal dendrites, and/or axon displayed a heavy immunolabeling to neuronal somata made faintly visible by a few small (<1 μm) immunoreactive particles in their cytoplasm (Tables 1, 2; Fig. 1). The cell nucleus was systematically unlabeled. It is to be emphasized that heavily and weakly staining neurons were often segregated in different nuclei or cell layers (Tables 1, 2). It is also of note that, although the heavily ReIn-ir neurons displayed solid labeling even in suboptimal experiments, many of the weakly ReIn-ir neurons were only evident in the nickel-enhanced immunostained

material. This qualitative observation suggests wide differences in Reelin protein content between immunoreactive neurons. We want to emphasize that the immunoreactivity in the cells that we describe as “weakly labeled” was far above background, and not weak in absolute terms, but only by comparison with the solid-black labeling of the neurons that we call “heavily” labeled (Fig. 1). Moreover, high-magnification analysis of the “weakly” labeled cells usually revealed small but heavily stained intracellular particles that were just too small to be seen at low magnification under bright-field optics. The analysis of labeled semithin sections counterstained with toluidine blue confirmed that the corpuscles surrounded the nucleus and often extended into the dendritic shafts and axon hillock (Fig. 1C). The light microscope appearance of these intracytoplasmic corpuscles is consistent with the possibility of Reelin immunolabeling in the endoplasmic reticulum and Golgi complex, as has been described recently by using electron microscopy in adult macaque (Martínez-Cerdeño et al., 2002) and mouse neurons (Pappas et al., 2002).

The axons of several ReIn-ir neuron populations were also immunolabeled (Fig. 1B–D), including those from neurons that gave rise to long axonal pathways. This immunolabeling consisted of discrete, very small (0.5–1 μm) bead-like corpuscles (Fig. 1D). Except for these specific axonal tracts, the remaining white matter was unlabeled.

In addition to labeled neuronal somata, most gray matter regions showed immunoreactivity in their neuropil. The intensity of this labeling fluctuated markedly among different nuclei and layers (Tables 1, 2). Examination of the neuropil labeling at high magnification showed that it consisted of both (a) a homogeneous background staining and (b) numerous discrete particles (<1 μm) or thin, discontinuously stained neurites.

Reelin immunoreactivity in the olfactory bulb

Several neuronal populations of the main olfactory bulb were conspicuously ReIn-ir (Fig. 1A–C). These include (1) most of the periglomerular neurons, (2) most of the tufted cells in the plexiform layer, (3) all the mitral cells, (4) a relatively small population of granular cells, and (5) occasional larger cells of the granular layer, presumably Cajal cells. In addition, the background neuropil immunoreactivity that was evident in all neuronal layers of the bulb was virtually absent from the olfactory glomeruli, as well as from the elongated clusters of granule cell somata (Fig. 1B).

Labeling of the mitral cells was particularly intense; remarkably, however, the labeling was limited to perikarya and axons, whereas the dendrites were only faintly immunoreactive and the cell nucleus was unlabeled (Fig. 1C). The mitral cell axons displayed a heavy but discontinuous labeling consisting of bead-like particles. These axons could be followed as they penetrated into the white matter stem of the olfactory bulb (Fig. 1C, arrowheads), where they joined the lateral olfactory tract (LOT). Many LOT axons displayed the same bead-like labeling (Fig. 1B,D).

Olfactory cortical areas

The various anterior olfactory nucleus (AON) subdivisions showed a similar pattern of labeling: in sharp con-

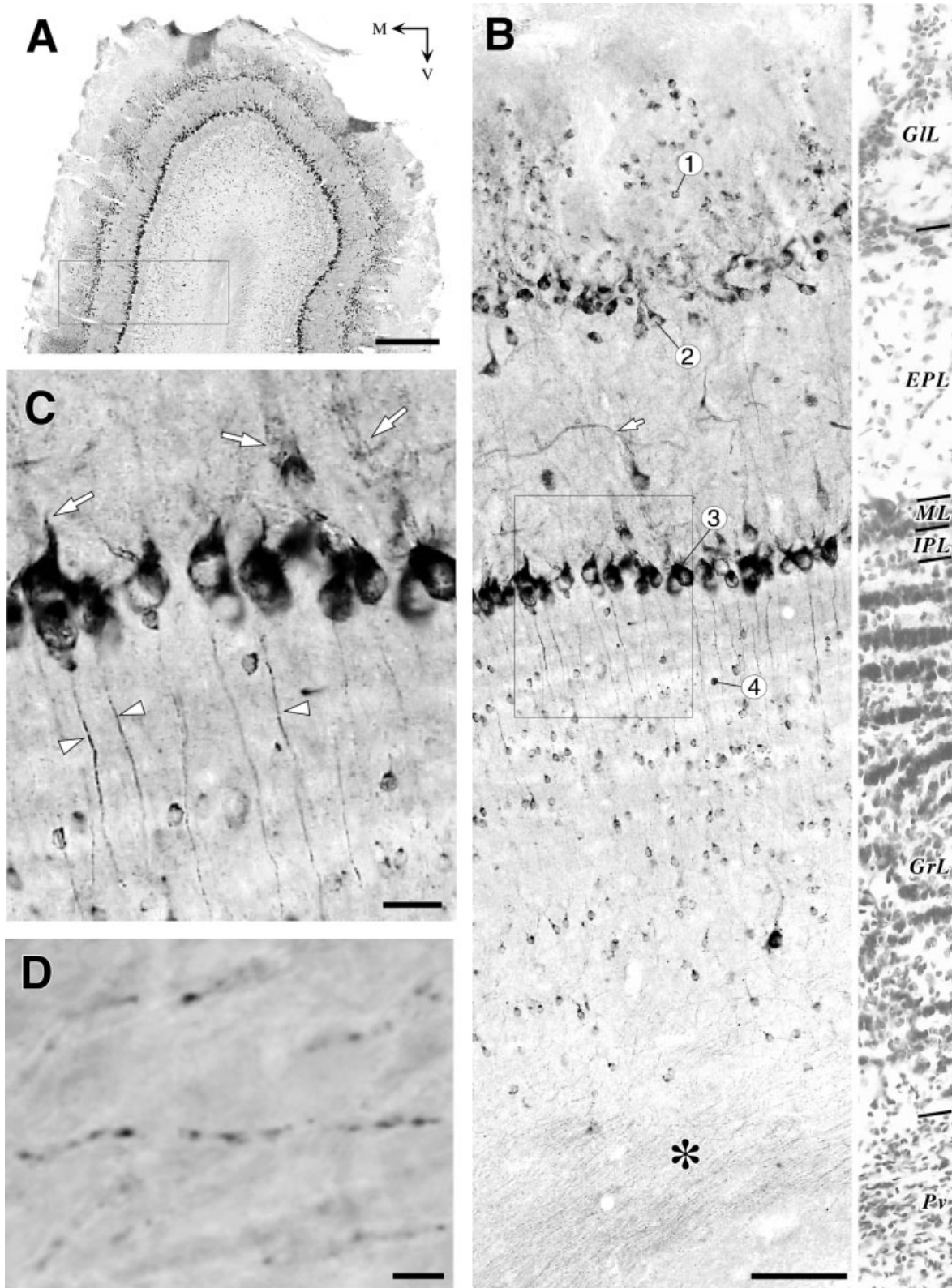


Fig. 1. Reelin-immunoreactive (ReIn-ir) neurons, axons, and neuropil in the main olfactory bulb. **A:** Panoramic view of a coronal section of the olfactory bulb. The M arrow points to medial, the V arrow to ventral. **B:** Immunolabeled periglomerular (1), tufted (2), mitral (3), and granular neurons (4). The area illustrated corresponds to the inset in A. Note the neuropil labeling that appears as a faint homogenous background and that is evident in the external and internal plexiform layers. For cytoarchitectonic reference, a sample from a parallel cresyl violet-stained section is attached on the right side of the panel. Comparison with the Nissl image shows that that, whereas virtually all the mitral cells, and most of the periglomerular and tufted cells are ReIn-ir, only small subpopulations of granular neurons are labeled. **C:** A high-magnification view of the mitral cells

reveals labeling in the proximal portions of the axons (arrowheads), with weak, incomplete immunolabeling of their apical dendrites (arrows). The area illustrated corresponds to the inset in B. Note that the initial axon segment and the axonal hillock of the mitral cells is only weakly labeled or unlabeled, whereas more distal parts of the axon are heavily immunoreactive. Notice also that the cytoplasm at the base of the apical dendrite is heavily immunoreactive. **D:** Immunoreactive axons in the lateral olfactory tract (sampled from the area indicated by an asterisk in B). At this high magnification, it can be easily appreciated that the axon labeling consists of numerous, relatively large (0.5–1.5 μm) bead-like particles. For abbreviations, see list. Scale bars = 500 μm in A, 100 μm in B, 25 μm in C, 5 μm in D.

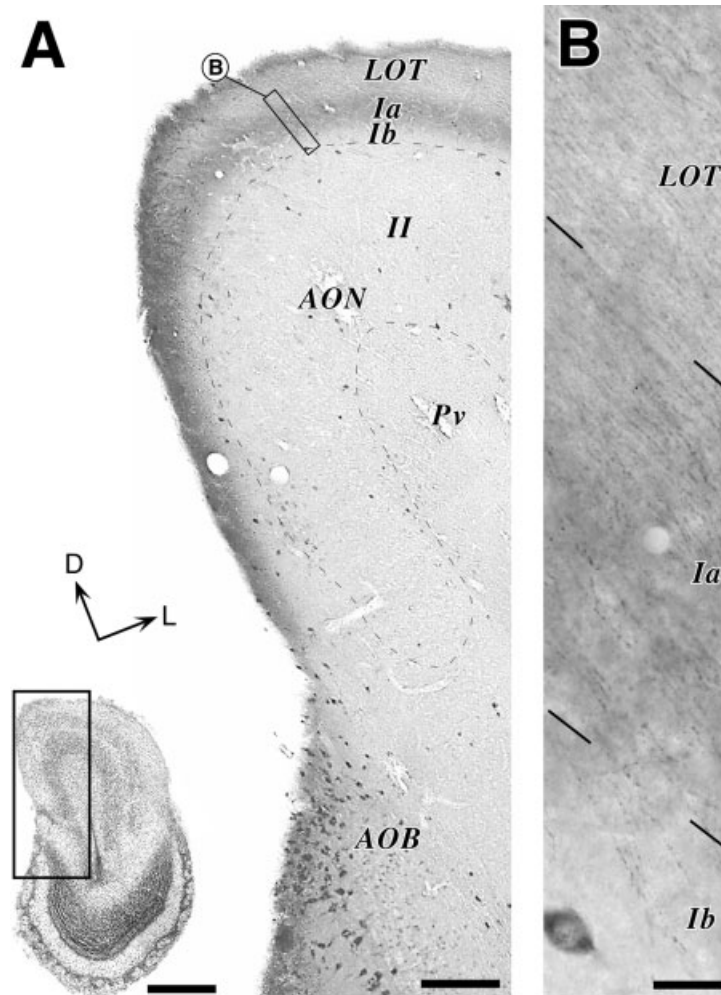


Fig. 2. Reelin-immunoreactive neurons, axons and neuropil in the anterior olfactory nucleus (AON). **A:** Reelin immunoreactivity in AON. For cytoarchitectonic orientation, a cresyl violet-stained coronal section of the olfactory bulb and its peduncle is shown at small scale in the lower left corner, and a rectangle indicates the area of immunostained tissue illustrated at larger magnification on the right. Note the heavy neuropil labeling in the superficial layer (layer I) and the labeling of axons in the lateral olfactory tract (LOT), despite the very low number of immunolabeled cell somata in AON. The D arrow

points to dorsal, the L arrow to lateral. **B:** High-magnification view (inset in A) of the labeling in the superficial layer of the AON. Observe that, although discrete immunoreactive axons are present in both LOT and AON, a dark band of homogeneous neuropil labeling, suggestive of extracellular Reelin, covers the outer layer of AON. This band matches the terminal field of LOT axons in AON (see text). For abbreviations, see list. Scale bars = 1 mm in A (left), 250 μm in A (right), 20 μm in B.

trast with the olfactory bulb, only occasional isolated cells were ReIn-ir (Fig. 2). These few cells were located in AON layers I and III, but not layer II, and they displayed fusiform or multipolar somata. Most LOT fibers displayed the same discontinuous bead-like labeling observed in more rostral levels. The outer half of AON layer I (sub-layer Ia, Price, 1973) contained a very heavy neuropil labeling (Fig. 2B). Of interest, this neuropil labeling decreased abruptly in the inner half of the layer (sublayer Ib). At high magnification, the labeling in layer Ia consisted of thin varicose neurites. These layer Ia neurites showed a staining identical to that seen in the LOT axons located superficially (Fig. 2B,C). Unlike LOT, however, the layer Ia labeling included a heavy background of homogeneous, presumably extracellular, protein. The Ib, II, and III layers of AON contained occasional ReIn-ir fibers.

Very much like the AON, the olfactory tuberculum (OT, Fig. 3A) and the nucleus of the lateral olfactory tract (NLOT, Fig. 3B) contained almost no ReIn-ir cells, although there was a band of heavy neuropil labeling in the outer half of its layer I (layer Ia, Price, 1973). In OT, this band showed prominent thickenings that, in thionin-counterstained sections, were found to lie between the islands of Calleja (compare Figs. 3A, 4A). A few occasional ReIn-ir neuronal somata were present in layers I and III; however, no cells were labeled in layer II (pyramidal layer) or in the islands of Calleja. The ReIn-ir cells were mainly fusiform or multipolar, and their proximal dendrites were made visible by the immunolabeling.

The pyriform cortex (PyC) contained numerous ReIn-ir cells in all its layers, but most prominently in layer II (pyramidal layer, Fig. 3A–D). Most of the neurons labeled

in PyC layer I were bipolar or fusiform, heavily staining, and most of them showed labeled dendrites that ran parallel to the pial surface. A band of heavily labeled neurons prominently delineated layer II (pyramidal layer). The proximal portions of the axons and dendrites of the ReIn-ir layer II cells were also immunolabeled (Fig. 3D,E). It should be noted that, in ferrets as in other mammals, this layer consists of several rows of similar, tightly packed pyramidal neurons (Krettek and Price, 1977; Haberly and Price, 1978). Remarkably, thionin counterstain revealed that the ReIn-ir neurons in this layer were only found in the superficial cellular rows of the layer, whereas the deeper cells in the layer were unlabeled (Fig. 4B,C). This sharply split pattern of ReIn-ir in layer II was visible throughout the lateromedial and rostrocaudal extent of the anterior and posterior pyriform areas (Figs. 3A–C, 4B,C). Layer III (multiform layer) of the PyC contained a substantial number of immunoreactive neuronal somata scattered throughout the layer. They were fusiform or multipolar, and they displayed diverse levels of staining.

The LOT fibers displayed bead-like immunolabeling identical to that noted in rostral portions of the same tract. In addition, a band of dark ReIn-ir neuropil lay along the outer half of layer I (sublayer Ia) throughout the anterior and posterior PyC (Figs. 3A–C, 4B,C). As observed in the AON, this neuropil immunolabeling decreased abruptly at the border between sublayers Ia and Ib, and it was markedly heavier than in the superficially adjacent LOT. As also in AON (Fig. 2B,C), at high magnification, the difference between LOT and sublayer Ia was found to consist not in a change of the density of immunoreactive fibers between strata but, rather, in the absence of the heavy, homogeneous, presumably extracellular, labeling in LOT that pervaded the PyC Ia sublayer neuropil. In contrast, sublayer Ib, and layers II, and III displayed weak neuropil immunoreactivity.

Other basal telencephalic structures

The various septal nuclei displayed markedly different labeling patterns (Fig. 5A–C). Many ReIn-ir neurons, some of which were heavily stained, were present in the medial septal nucleus. Some of these cells were adjacent to the pia, and their proximal dendrites were stained along a considerable length. Clusters of similar neurons delineated both the vertical and horizontal nuclei of the diagonal band (Fig. 3A). In the intermediate division of the lateral septal nucleus, virtually all neurons were immunoreactive; nevertheless, the staining of neuronal somata was markedly weaker than in the medial nucleus, and the dendrites of these neurons were not labeled (Fig. 4B). In contrast, the laterodorsal and intermediate septal nuclei were mostly unlabeled. Neuropil labeling was visible in all nuclei but most intense in the medial nucleus.

Across the striatum, the intensity of immunostaining was quite low overall. At higher magnification, it was evident that a large majority of the striatal neurons were ReIn-ir, although most of them contained just some few very small ($< 1 \mu\text{m}$) stained particles in their perikaryon (Fig. 5D). Occasional striatal cells displayed similar but more robustly labeled particles (Fig. 5E). In the rostromedial caudate nucleus and in the nucleus accumbens, the neurons in some small patch-like domains of tissue stained slightly more intensely than those in the adjacent zones (Fig. 5D). Weak neuropil immunoreactivity was detectable throughout the striatum.

Few cells were labeled in the lateral and ventral pallida (Fig. 3A,B). In the lateral pallidum, the labeled cells were multipolar, large (10–15 μm main diameter), and weakly staining. The occasional cells labeled in the ventral pallidum were smaller (5–10 μm) and stained more darkly.

Each of the amygdala nuclei contained a population of ReIn-ir cells (Fig. 5F). In the lateral, basal, accessory basal, and central amygdaloid nuclei, the labeled neurons were fusiform, or multipolar, and relatively small (5–7 μm). Numerous cells with a similar appearance were immunolabeled in the substantia innominata and in the anterior amygdaloid areas (Fig. 3B). The observation in thionin-counterstained sections (not shown) that the larger neurons in all the above nuclei were not immunoreactive suggests that most of the ReIn-ir amygdala neurons might be interneurons. Neuropil immunoreactivity was low throughout the amygdaloid complex, except in the subpial portion of the cortical nucleus, where it was relatively heavy (Fig. 5F).

Virtually all the axons of the stria terminalis (not shown) were robustly ReIn-ir. As in other fiber tracts, the labeling of these axons consisted of small ($< 0.5\text{--}1 \mu\text{m}$), discrete immunoreactive particles. In addition, a few heavily immunostained neurons were occasionally present in the bed nucleus of the stria terminalis.

Hippocampal formation and parahippocampal cortex

Several populations of cells in the hippocampal formation were heavily ReIn-ir (Fig. 6); in all cases, their morphology and laminar position were those of interneurons. The granular cells of the dentate gyrus (Figs. 4G, 6B), as well as the pyramidal cells of Ammon's horn (Fig. 6C) and the subiculum (Fig. 6A) were not labeled.

Numerous large multipolar somata and their proximal dendrites were labeled in the plexiform layer of the dentate gyrus (DG, Figs. 4G, 6B). Occasional smaller cells were stained in the molecular layer of this area, but granular neurons were unstained. Neuropil labeling was the heaviest near the pial/hippocampal fissure border in the molecular layer (ML, Fig. 6A,B).

The various sectors of Ammon's horn displayed a similar pattern of immunolabeled cells: (1) large heavily staining bipolar or multipolar cells with smooth, mostly tangential dendrites in the stratum lacunosum moleculare, (2) a few cells with the appearance of interneurons in the stratum radiatum and stratum pyramidale, and (3) smaller fusiform cells in the stratum oriens (Fig. 6A,C). In addition, a prominent band of heavily immunoreactive neuropil delineated the stratum lacunosum moleculare. This neuropil labeling decreased abruptly at the border with the stratum oriens. In addition to the homogeneous background, this neuropil included numerous immunoreactive puncta. Moreover, it contained thick immunolabeled neurites that were oriented in different directions and often seemed to be continuous with the dendrites of large labeled interneurons in this stratum.

The labeling pattern in the subiculum was similar to that in Ammon's horn. In contrast, the parasubiculum and prosubiculum contained markedly fewer labeled cells in layer I, and more ReIn-ir neurons in layers II–V (Fig. 6A). The fusiform shape and small soma size ($\sim 5 \mu\text{m}$) of the ReIn-ir cells in the subicular complex indicated that they

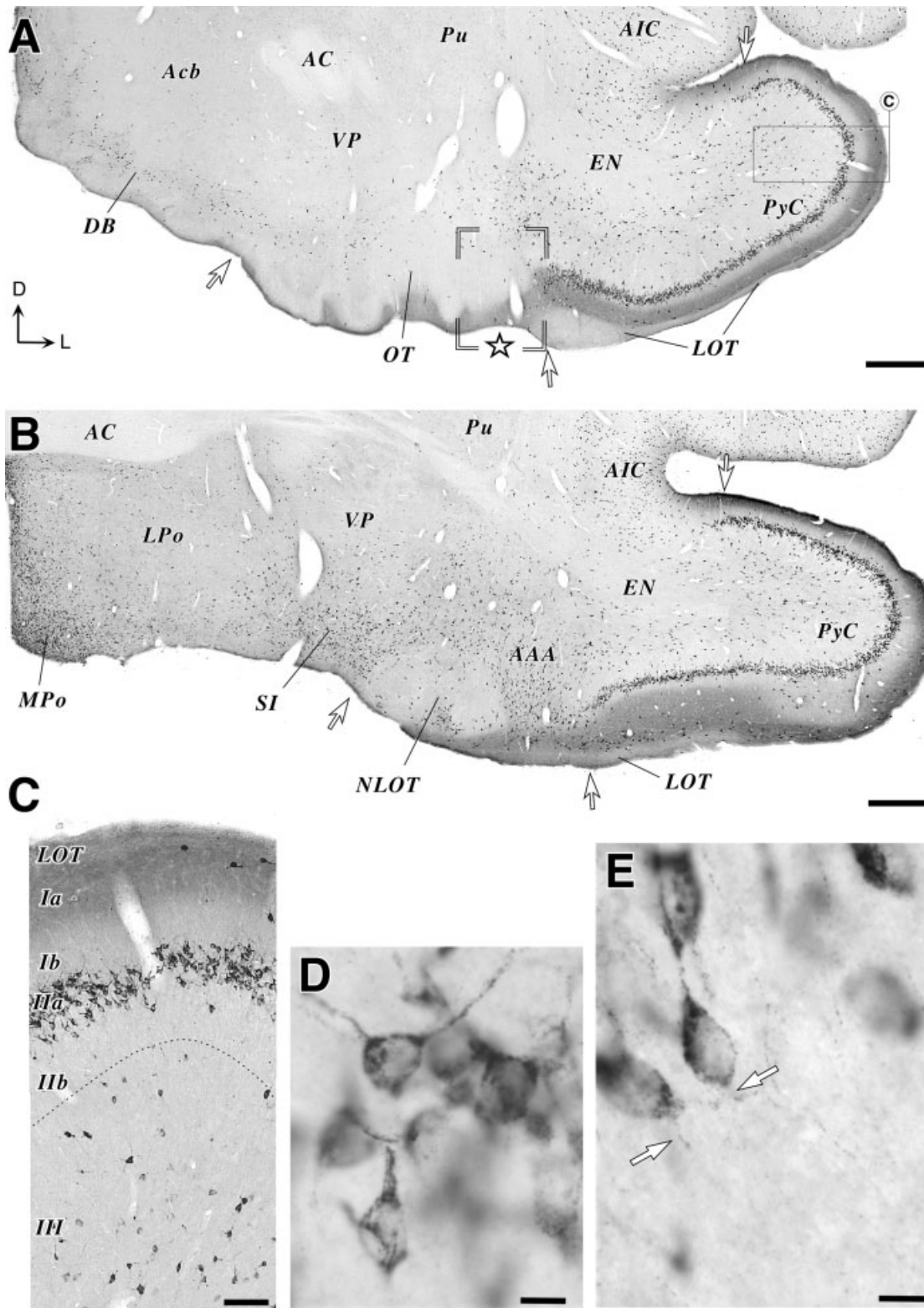


Figure 3

were mainly interneurons, an observation confirmed in thionin-counterstained sections by the absence of labeling in the pyramidal cells.

All the layers of the entorhinal cortex contained numerous immunolabeled small neurons of fusiform or multipolar shape. In addition, large numbers of pyramidal cells were heavily labeled in layer II (Fig. 6A,D), whereas additional, more weakly labeled pyramidal cells were present in layer III. In fact, thionin counterstain (Fig. 4D–E) revealed that most of the layer II cells were ReIn-ir, except for a few isolated clusters of tightly packed cells in the lower zone of the layer. Moreover, some differences were noticeable between the various entorhinal areas in the relative number and distribution of these ReIn-ir pyramidal layer II cells (Figs. 4F, 6A).

An unexpected finding was that virtually all the axons of the ReIn-ir layer II entorhinal cells were highly immunoreactive (Fig. 6E), and displayed the discontinuous, bead-like pattern of staining already noted in some other axonal tracts (see above). In coronal sections, these axons were seen leaving the cell somata and could be followed for some hundred microns as they continued into the white matter of the parahippocampal gyrus (the so-called angular bundle). They formed a patent, ReIn-ir, fiber stratum within the angular bundle (Fig. 6A,D,F). Interestingly, numerous immunoreactive axon fascicles were seen leaving this stratum to traverse the cellular layers of the subiculum toward the hippocampal fissure (Fig. 6G). It is to be noted that, in carnivores as in other mammals, layer II entorhinal cell axons are known to traverse the subiculum in small fascicles to arborize in the lacunosum moleculare stratum of CA and outer third of DG molecular layer (Witter and Groenewegen, 1984). As mentioned above, the neuropil of these layers is heavily ReIn-ir (Fig. 6A). Taken together, these observations indicate that most, if not all, of the cells of origin, axonal trunks and terminal arborizations of the entorhinohippocampal (“perforant”) pathway are heavily immunoreactive for Reelin in ferrets. An important implication of this finding is that the axons of the entorhinohippocampal pathway may secrete substantial amounts of Reelin in the extracellular matrix of the CA and DG molecular layers.

Neuropil immunolabeling was present in all the layers of the entorhinal cortex, but it was particularly heavy in the subpial zone of layer I. It is to be noted that this labeling is roughly coextensive with the known terminal

field of LOT axons in the entorhinal cortex of carnivores (Room et al., 1984).

Isocortical areas

The pattern of Reelin immunolabeling was remarkably homogeneous across the isocortex (Fig. 7). All layers contained numerous ReIn-ir neurons, but the relatively most abundant and heavily stained population was located in layers I and II (Fig. 7A,B). These neurons ranged 7–12 μm in soma diameter, and their morphology, including their proximal dendritic trees, was clearly revealed by the immunolabeling (Fig. 7B,C). Although we did not investigate whether the heavily ReIn-ir neurons of isocortical layers I–II constituted one or more neuron populations, for descriptive purposes, we grouped them into three main morphologic types: (a) neurons with a pear-shaped body that bulged on the cortical surface (Fig. 7B) and had a single, thick, descending dendrite with several right-angled second-order branches; (b) subpial, heavily ReIn-ir cells that displayed one or two smooth, tangentially oriented dendrites; (c) large multipolar neurons (Fig. 7C). Cells of types “a” and “b” were situated in the superficial half of layer I, whereas “c” cells were located in the lower half of the layer and in layer II; in addition, numerous smaller (5–7 μm in soma size) and usually more weakly labeled cells (labeled “d” in Fig. 7B) of bipolar shape were present in the lower half of layer I and in all of layer II.

Isocortical layers III–VI contained some heavily immunoreactive neurons; however, most neurons labeled in these layers were weakly stained. The small size (5–7 μm) and bipolar or multipolar shape of these neurons indicates that they were interneurons. Overall, layers II and V contained the highest density of these ReIn-ir interneurons (Fig. 7A). As a rule, virtually none of the isocortical pyramidal cells were immunoreactive for Reelin, an observation confirmed by thionin counterstaining; however, a few weakly ReIn-ir layer V pyramidal cells were consistently observed in some isocortical areas (Fig. 7A,B). Neuropil labeling was present in all cortical layers but markedly more dense in the subpial portion of layer I (Fig. 7A).

Dorsal thalamus and epithalamus

Numerous neurons in all the nuclei of the dorsal thalamus were ReIn-ir (Figs. 8, 9). Intriguingly, the relative amounts of these cells in the different nuclei was quite variable. They were scarce in certain portions of nuclei

Fig. 3. Reelin-immunoreactive neurons, axons, and neuropil in olfactory and other basal telencephalic regions. **A,B**: Panoramic views of immunostained coronal sections of the basal telencephalon. The D arrow points to dorsal and the L arrow to lateral. The sections were taken at 8.0 mm (A) and 6.4 mm (B) rostral to the interaural plane, respectively. Open arrows indicate the approximate location of borders between cortical areas. At this low magnification, it can be readily appreciated that the heavily immunoreactive (dark) neurons are mainly restricted to the pyriform cortex (PyC), the diagonal band nuclei (DB), substantia innominata (SI), the anterior amygdaloid area (AAA), and the medial preoptic area (MPo), whereas they are absent in other regions. The neuropil in the superficial part of layer I in the pyriform cortex, olfactory tuberculum, and nucleus of the lateral olfactory tract are very heavily immunostained. The LOT is also immunolabeled, although its staining intensity is lower than that of the neuropil in subjacent layer I. **C**: Detail of the labeling corresponding to the thin line inset in A. The pial surface is toward the top. The

population of Reelin-positive neurons is sharply restricted to the outer half of the pyramidal layer (layer IIa). The inner half of the pyramidal layer is unlabeled. For reference, a dashed line delineates the border between layers IIb and III. Notice that, in addition to the pyramidal cells labeled in layer IIa, some neurons are immunolabeled in layer III and I. **D,E**: High-magnification views of the immunolabeled pyramidal neurons in layer IIa. Most of the neurons, particularly those situated more superficially within layer IIa, typically display a bitufted dendritic arrangement, whereas deeper neurons show a single apical dendrite. The perikaryon and proximal dendrites of these ReIn-ir neurons display immunoreactive corpuscles whose appearance and distribution is suggestive of labeling in the endoplasmic reticulum and Golgi complex. The axons of these pyramidal neurons (arrows in D) are visible as rosaries of immunolabeled particles. For other abbreviations, see list. Scale bars = 500 μm in A,B, 100 μm in C, 10 μm in D,E.

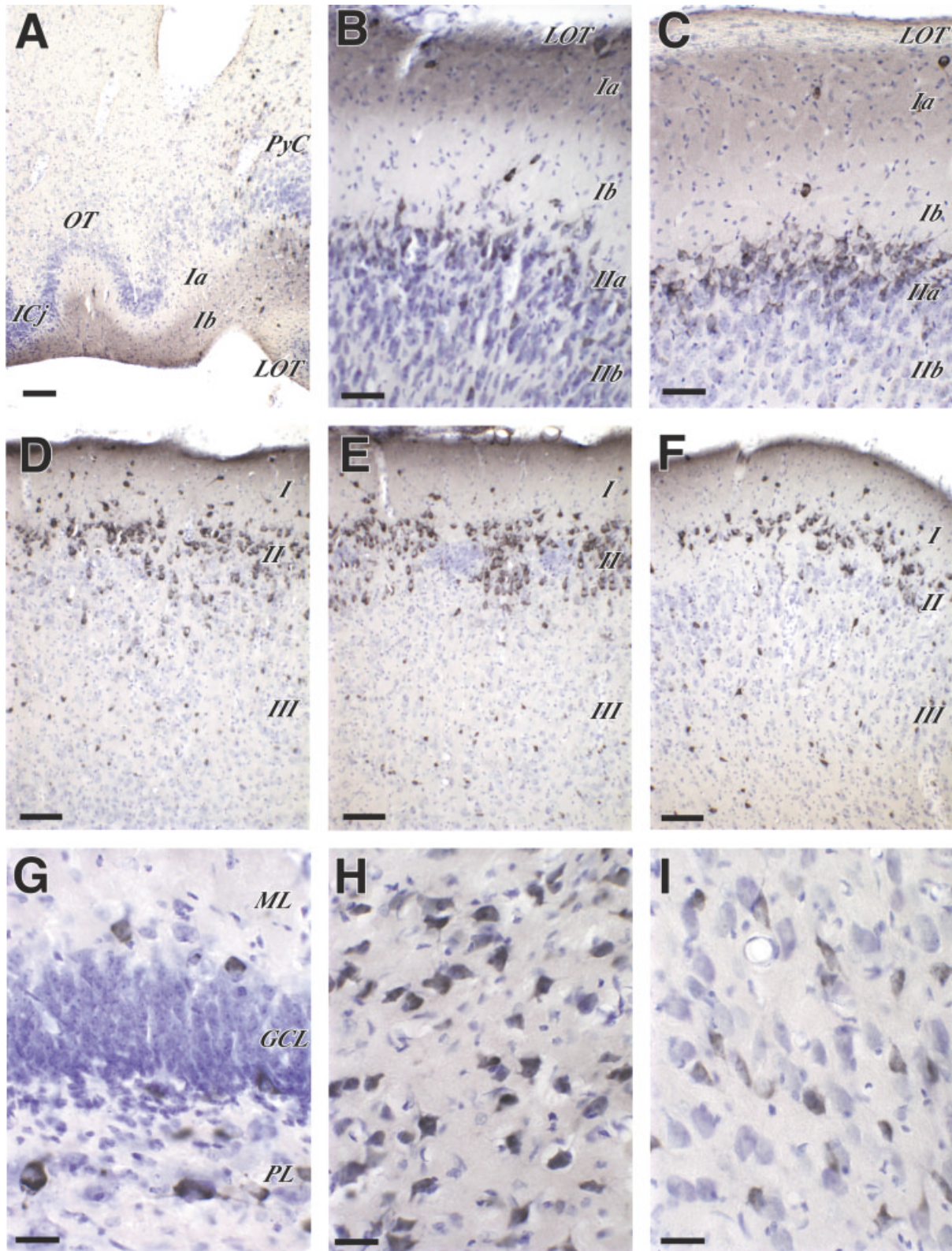


Fig. 4. Selective localization of Reelin immunoreactivity to discrete neuronal subpopulations and neuropil compartments. Immunostained sections with cresyl violet counterstain. **A:** Olfactory tubercle and adjacent pyriform cortex. For orientation, a comparable area is indicated by an open double-line rectangle labeled with a star in Figure 3A. The basal surface of the brain is toward the bottom. **B,C:** Layers I-II of the pyriform cortex in an anterior and posterior region of this cortex, respectively. Note that the immunolabeled neurons are a subpopulation of the pyramidal cells in layer II, and most of them are situated in the superficial part of the layer (sublayer IIa). Note also the occasional cells labeled in layer I, and the abrupt difference in neuropil labeling between the outer and inner halves of layer I (sublayers Ia and Ib, see text). **D,E:** Layers I-III of the entorhinal cortex. The pial surface is at the top. **D:** Medial entorhinal area.

E: Lateral entorhinal area. **F:** Dorsolateral entorhinal area. Note that, whereas the relative number and position of cells in layers I and III is similar in all three entorhinal areas, the labeled and unlabeled cells in layer II display a characteristic arrangement in each area. **G:** High-magnification view of the dentate gyrus. The pial surface or hippocampal fissure is situated toward the top. Notice the presence of immunoreactive interneurons just above (molecular layer, ML) and below (plexiform layer, PL) the granular layer (GCL) and the absence of labeled neurons in the GCL. **H:** Reuniens thalamus. **I:** Lateral posterior nucleus of the thalamus. Comparison of H and I reveals that, whereas virtually all the large projection neurons in the reuniens are immunoreactive, only a subpopulation of the large neurons in the lateral posterior nucleus contains Reelin. For other abbreviations, see list. Scale bars = 100 μm in A, 50 μm in B,C, 100 μm in D,E, 25 μm in G-I.

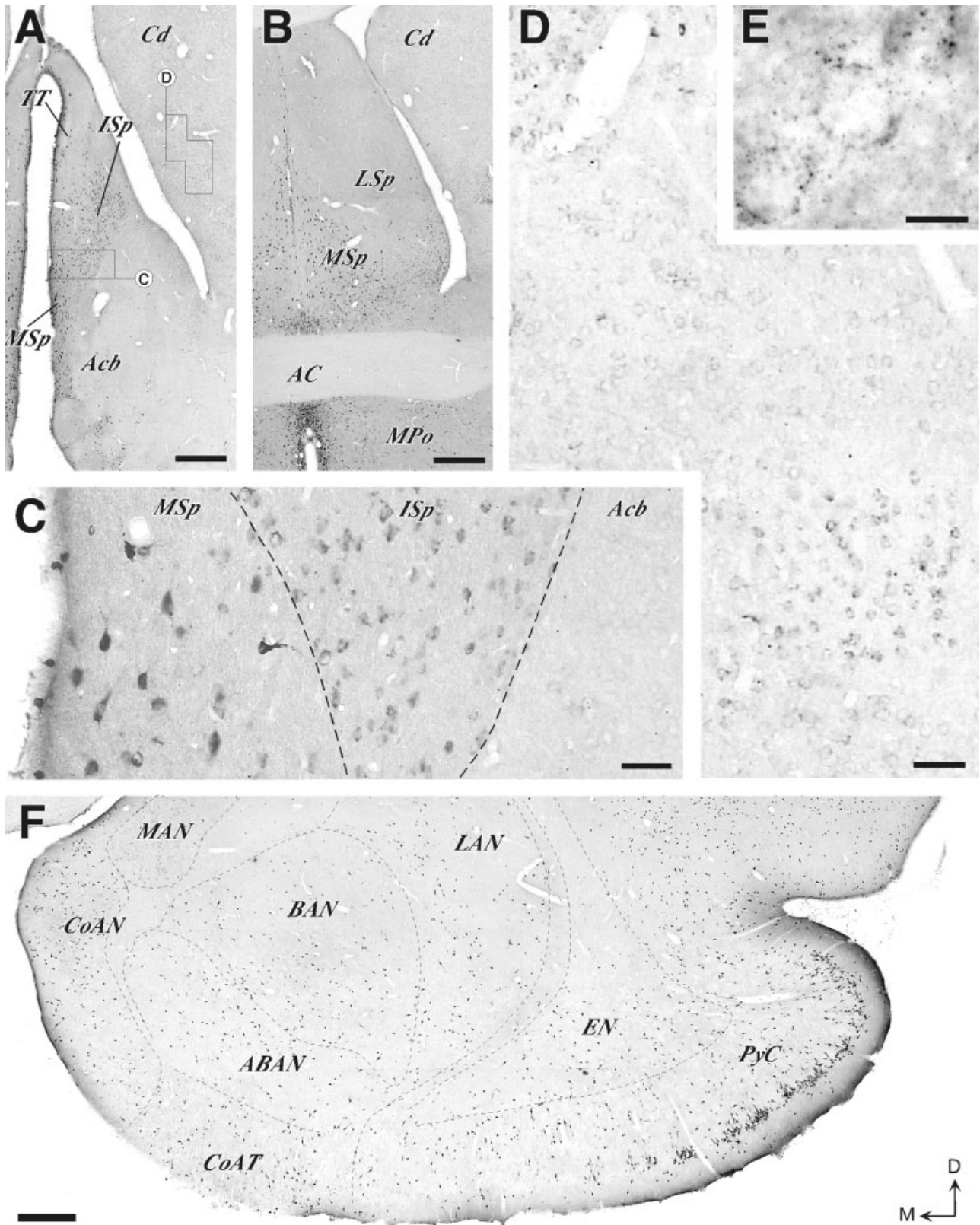


Fig. 5. Reelin-immunoreactive neurons and neuropil in the septal, striatal, and amygdaloid nuclei. **A,B:** Panoramic view of two coronal sections of the septal nuclei and adjacent regions. Sections correspond to the coronal level shown in Figure 3A,B. Note the abundant labeled neuronal somata in the medial (MSp) and intermediate septal (ISp) nuclei. **C:** Detail of the labeling in MSp and ISp and in the adjacent nucleus accumbens (Acb, inset in A). Dashed lines indicate nuclei borders. Observe that, in each of these three nuclei, the neurons display markedly different levels of Reelin immunoreactivity. **D,E:** Reelin-immunoreactive neuronal bodies in the caudate nucleus. **D:** Illustrated is detail of the head of the caudate (inset in A) for which virtually all striatal cells are immunoreactive, although weakly.

Moreover, the cells in some tissue domains are slightly more immunoreactive than others. **E:** At high magnification, the labeling can be seen to consist of small intracellular corpuscles surrounding the cell nucleus. **F:** Panoramic view of labeling in the amygdaloid complex and adjacent pyriform cortex. Note that heavily immunolabeled cells are present in all amygdaloid nuclei, except in the medial nucleus (MAN), which contains only weakly, but numerous, labeled cells. Note also the heavy subplial neuropil labeling of the pyriform cortex (PyC). The D arrow points to dorsal, the M arrow to medial. For other abbreviations, see list. Scale bars = 500 μ m in A,B,F, 50 μ m in C,D, 10 μ m in E.

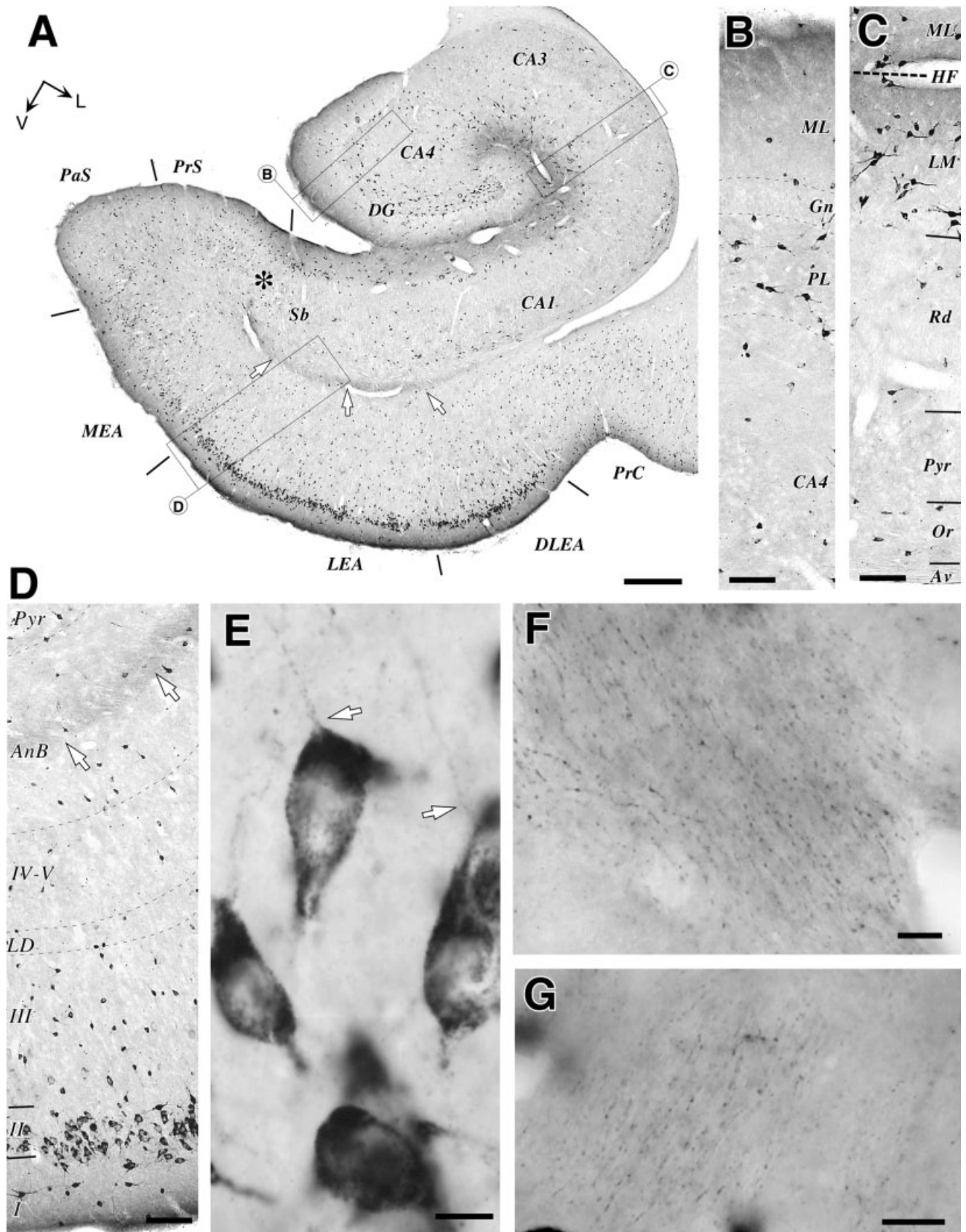


Figure 6

such as the parataenial (Fig. 8A) or mediadorsal but very numerous in other nuclei such as the reuniens thalami anteroventral, posterior, medial geniculate (Fig. 10A) dorsal lateral geniculate, and lateral posterior (Fig. 9A,B). In the dorsal lateral geniculate (Fig. 9F), neurons in the magnocellular "C" layer were slightly more intensely stained than neurons in sublayers "A" and "A1" (Linden et al., 1981). Thionin counterstaining revealed that in most thalamic nuclei the ReIn-ir neurons were small and medium stellate and multipolar cells, whereas many of the largest thalamic neurons were unstained (Fig. 4I). However, in other nuclei such as the reuniens (Fig. 4H) virtually all the neurons, including the larger ones, were ReIn-ir. Neuropil labeling was present throughout the dorsal thalamus, with slight differences in intensity between the various nuclei (Figs. 4H,I, 8A, 9A).

Most cells in the habenular nuclei were heavily ReIn-ir (Fig. 9A,C). The perikarya and a large proximal portion of their dendrites were immunolabeled. Of interest, most axons in the retroflex bundle (Fig. 9A,E) as well as the neuropil in the interpeduncular nucleus of the mesencephalon, which is the main target of the habenular axons, are ReIn-ir as well (Fig. 10A). Thus, very much as we pointed out in the axons of the LOT, stria terminalis and entorhinohippocampal pathway, these observations indicate that the habenular cells axons traveling the retroflex bundle may secrete substantial amounts of Reelin into the extracellular matrix of the interpeduncular nucleus.

Ventral thalamus and hypothalamus

In sharp contrast with the adjacent nuclei of the dorsal thalamus, the zona incerta and the reticular thalamic nucleus contained very few ReIn-ir neurons (Figs. 8A, 9A). Most cells in the ventral lateral geniculate nucleus were immunoreactive, although markedly less intensely so than cells in the adjacent dorsal lateral geniculate nucleus of the thalamus. The entopeduncular and the subthalamic nuclei contained scattered groups of immunoreactive cells. These cells were relatively large (12–20 μm soma diameter) and multipolar or fusiform (Fig. 9A).

The preoptic region, particularly the medial preoptic area, contained large numbers of heavily ReIn-ir cells (Fig.

3B). In the hypothalamus, the paraventricular nucleus was clearly delineated by the heavy immunolabeling of its neurons (Fig. 8A). The proximal dendrites and axons of these neurons were also labeled (Fig. 8C); again, the axon labeling consisted of discrete particles suggestive of secretory vesicles. The remaining nuclei and areas of the hypothalamus contained scattered ReIn-ir neurons, most of them weakly stained (Fig. 8A).

Pretectum and mesencephalon

Virtually all the neurons in a small nucleus of the pre-tectal region, the lateral nucleus of the posterior commissure, were heavily immunoreactive (Fig. 9A,D). Other pre-tectal nuclei contained many, although less heavily, stained cells (Fig. 9A).

The superior colliculus contained large numbers of ReIn-ir cells in all its layers but particularly in the stratum zonale (Fig. 10A,B). Throughout the collicular layers, the labeled cells were mainly of small and medium size (5–12 μm), although the intermediate and deep gray layers contained, in addition, some large, weakly ReIn-ir neurons (Fig. 10B,C). The neuropil of the stratum zonale was heavily ReIn-ir, and densest at the pial surface. It is interesting to note that this heavily labeled neuropil strictly matches the distribution of the terminal arborizations of retinal axons in the superior colliculus of ferrets (Zhang and Hoffmann, 1993).

Clustered groups of cells in the substantia nigra pars reticulata were ReIn-ir, whereas the rest of this nucleus contained few labeled cells (Fig. 10A,E). Virtually all neurons in the terminal nuclei of the accessory optic system were ReIn-ir (Fig. 10D). Other ReIn-ir mesencephalic neuron populations were located in the inferior colliculus (not shown), the dorsal and lateral portions of the periaqueductal gray matter (Figs. 10A, 11A), as well as in the reticular and raphe nuclei (Table 2; Figs. 10A, 11A).

Rostral brainstem and cerebellum

Reelin immunolabeling in the pons and medulla was overall markedly less abundant and more restricted than in the mesencephalon or forebrain (Table 2, compare Figs. 11A–C and 12 with Figs. 6–10). Nevertheless, numerous

Fig. 6. Reelin-immunoreactive (ReIn-ir) neurons, axons, and neuropil in the hippocampus and parahippocampal cortex. **A:** Panoramic view of the labeling in a coronal section of the temporal hippocampus at the level of the interaural plane. Note the marked differences in the distribution of labeled neuronal somata and neuropil between the various areas and layers. The thin, lettered rectangles indicate the areas shown at higher magnification in the following panels. Notice that a band of neuropil labeling covers the superficial layer of the subiculum (Sb), Ammon's horn sectors 1 and 3 (CA1, CA3), and of the dentate gyrus (DG). This neuropil labeling exactly matches the known distribution of the entorhinohippocampal (perforant) pathway. Notice also the prominent band of ReIn-ir fibers in the angular bundle of the temporal white matter (AnB, arrows). The V arrow points to ventral, and the L arrow to lateral. **B:** Laminar distribution of the immunolabeling in the DG (inset in A). Note that cells are relatively scarce in the molecular layer (ML) and absent from the granule cell layer (marked by a dashed line) but very abundant in the plexiform layer. Compare with Figure 4G. **C:** Laminar distribution of the labeling in CA3, corresponding to the inset in A. Note the large neurons with long, mainly tangential, dendrites present in the stratum lacunosum moleculare (LM). Smaller ReIn-ir neurons are present in LM and in the strata radiatum (Rd) and oriens (Or). Hippocampal pyramidal cells are nonimmunoreactive in ferrets. Notice that the heavy

neuropil labeling in LM is densest near the hippocampal fissure (HF), as well as in the apposed ML of DG. **D,E:** Immunoreactivity in the neurons of origin and axons of the entorhinohippocampal ("perforant") pathway. **D:** Laminar distribution of the labeling in the entorhinal cortex. Virtually all of the relatively large pyramidal cells in layer II are heavily immunoreactive. Compare with Figure 4D,E. Note that some additional pyramidal cells are weakly immunolabeled in layer III. Smaller interneuron-like neurons are also heavily labeled, particularly in layers I and III, but also in layers IV–V, and in the subcortical white matter of the parahippocampal gyrus (angular bundle, AnB). Note also the immunoreactive fibers in AnB (arrows). **E:** High-magnification detail of ReIn-ir pyramidal cells in entorhinal cortex layer II. In addition to the intracellular particles in the cell perikaryon and dendritic shafts, notice the presence of discrete immunolabeled particles in the axons leaving these cells (arrowheads). **F:** Large numbers of axons in the angular bundle are visible as rows of ReIn-ir particles. **G:** Detail of one of the numerous small bundles of ReIn-ir axons that can be seen traversing the pyramidal stratum of Sb. Such bundles are a distinctive feature of the perforant pathway. For orientation, the point at which this high-magnification image was taken is indicated by an asterisk in A. For other abbreviations, see list. Scale bars = 500 μm in A, 100 μm in B–D, 10 μm in E–G.

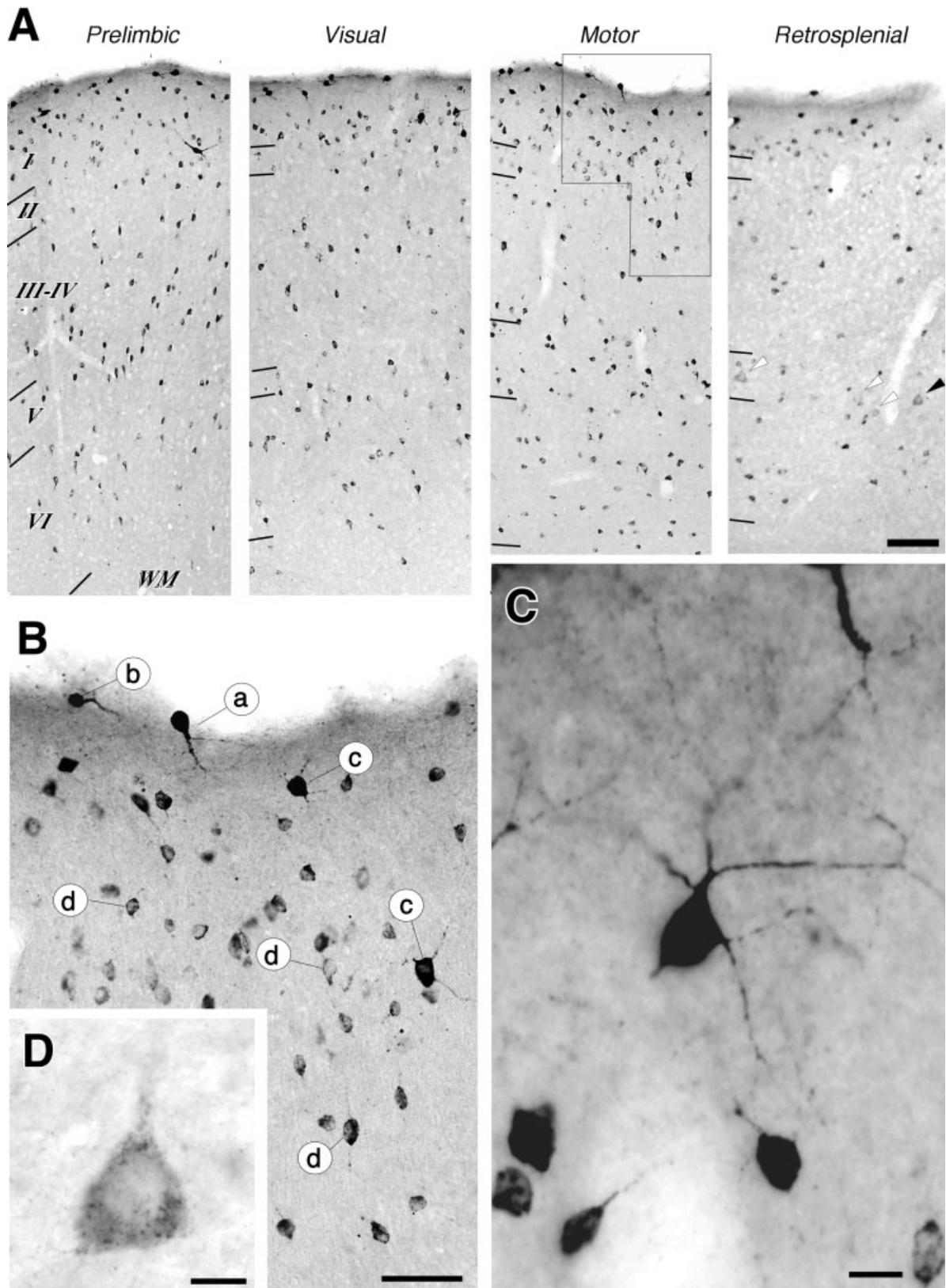


Fig. 7. Reelin-immunoreactive neurons and neuropil in the isocortex. **A:** Laminar distribution of the immunolabeling in samples taken from coronal sections of four isocortical areas. Interneuron-like neurons are numerous in all the layers, but particularly so in layer I. The sample from the retrosplenial cortex also shows some immunoreactive layer V pyramidal cells (arrowheads). **B:** High-magnification view of a retrosplenial cortex layer V pyramidal. The cell is the same one indicated with a black arrowhead in A. Notice that, as in other cells, the immunolabeled particles in the cell soma are located in the perikaryon and spare the cell nucleus. **C:** Detail of the labeling in

layers I-II of the motor cortex (lined inset in A). Note the diverse cell morphology and staining intensity of the various immunoreactive neurons. See text for a description of the cell types (identified here with letters a through d). High-magnification detail of interneurons in the inner half of layer I. Note the extensive dendrite immunolabeling in a large, heavily stained multipolar neuron (top). Three smaller weakly stained interneurons are situated at the border between layers I and II (bottom). M, medial; D, dorsal. Scale bars = 100 μ m in A, 10 μ m in B,D, 50 μ m in C.

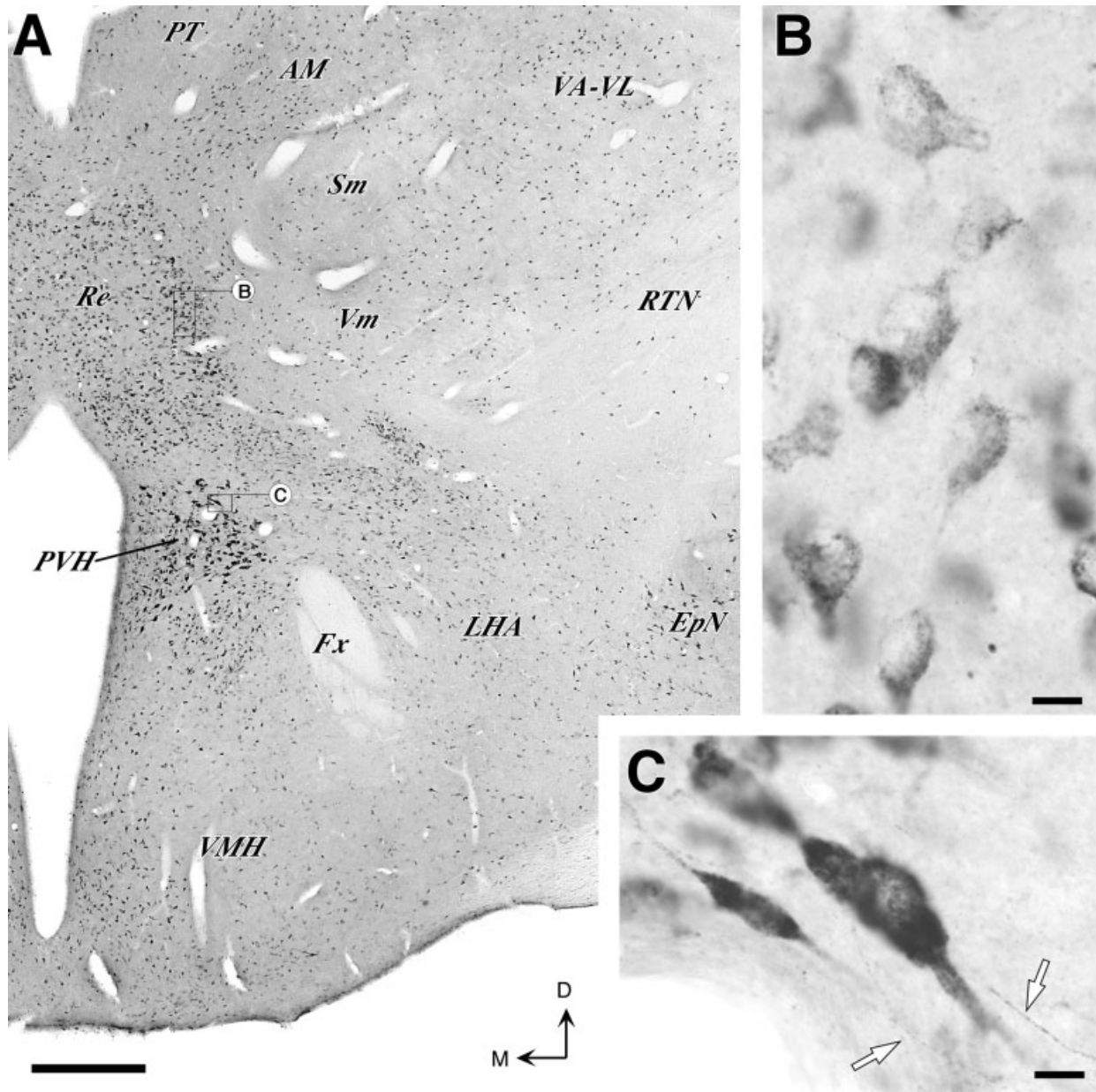


Fig. 8. Reelin-immunoreactive neurons and neuropil in the rostral thalamus and hypothalamus. **A:** Panoramic view of the immunolabeling in a coronal section taken 4.2 mm rostral to the interaural plane. Note the differences in cell density and staining intensity in the various nuclei. The heavy labeling of their neurons clearly delineates the paraventricular hypothalamic nucleus (PVH) and the reuniens thalami nucleus (Re). The presence of a substantial level of neuropil immunoreactivity throughout the gray matter of the hypothalamus

and thalamus is highlighted by the absence of labeling in the retro-commissural fornix (Fx). The parataenial (PT) and the reticular thalamic (RTN) nuclei contain only occasional labeled neurons. The D arrow points to dorsal, and the M arrow to medial. **B:** High-magnification detail of the labeled neurons in Re. **C:** High-magnification detail of the labeled neurons in PVH. Note that immunoreactive particles delineate their axons (arrowhead in C). For other abbreviations, see list. Scale bars = 500 μ m in A, 10 μ m in B,C.

Reln-ir neurons were still observed in the raphe nuclei (Figs. 10A, 11A, 12A,B) the principal trigeminal nucleus (Fig. 11B), the pontine nuclei (Fig. 12A), the superior olivary nucleus (Fig. 12A), and the lateral reticular nucleus (Fig. 12B). The motoneurons in the motor trigeminal (Fig. 11B,C) and hypoglossal nuclei (Fig. 12B) were also heavily Reln-ir, whereas those in the oculomotor and facial nuclei showed only very weak or no labeling. In addition,

the neuropil in some nuclei such as the pontine and the inferior olivary was clearly immunoreactive (Fig. 12).

The cerebellar cortex displayed heavy labeling in the granular cell layer. As in other neurons, this labeling consisted of discrete small perikaryal corpuscles, whereas the nucleus was unlabeled. Presumably due to the scant cytoplasm in these neurons, the individual somata were incompletely delineated by the immunolabeling (Fig. 11B)

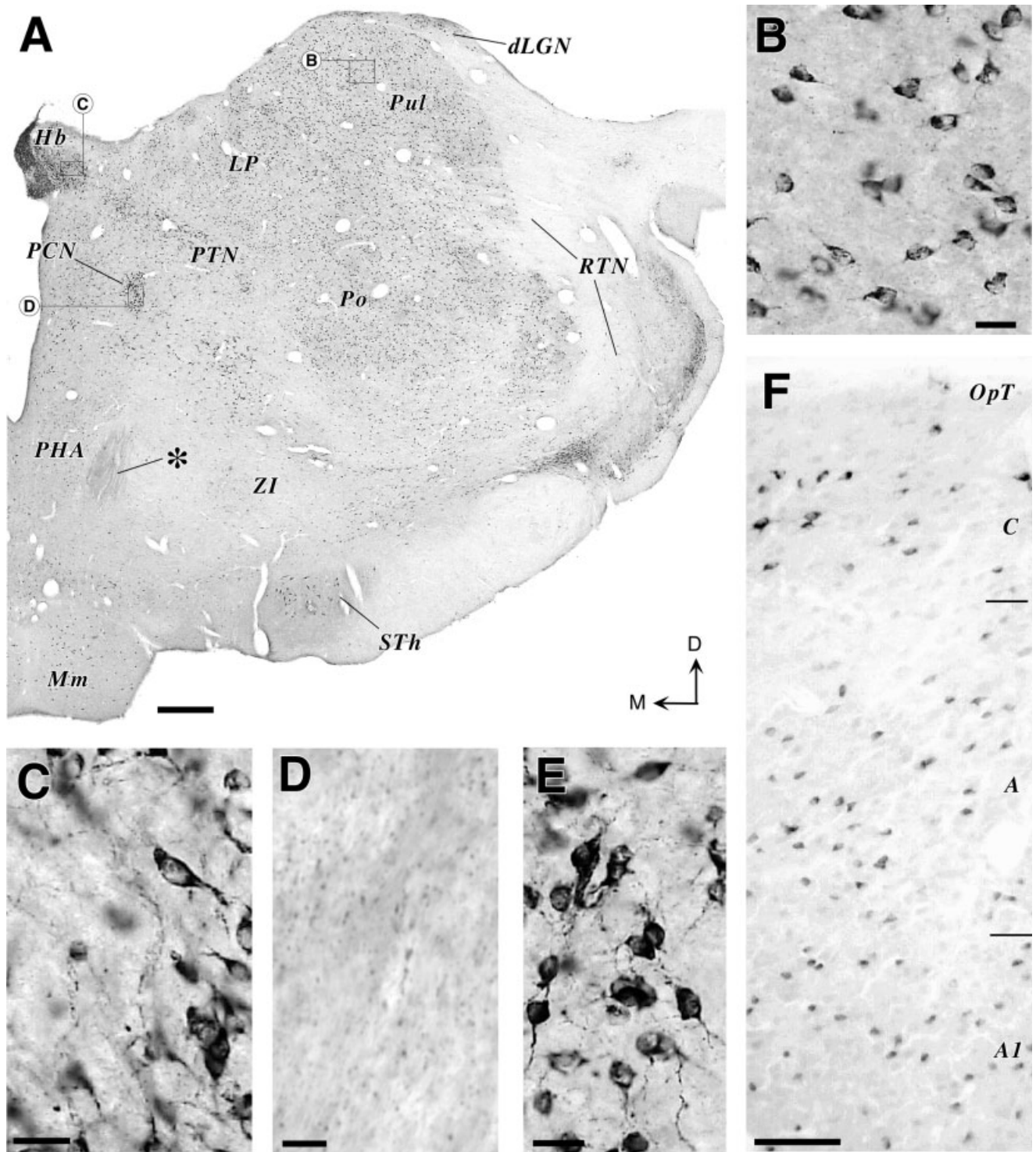


Fig. 9. Reelin-immunoreactive (ReIn-ir) neurons, axonal tracts and neuropil in the caudal diencephalon and pretectum. **A:** Panoramic view of an immunostained section taken at the interaural coronal plane. Large numbers of immunolabeled cells are present in the various thalamic nuclei, the habenular complex, and pretectum. In contrast, the mamillary nuclei (Mm), the posterior hypothalamic area (PHA), zona incerta (ZI), and subthalamic nucleus (STh) contain few ReIn-ir cells. Note that most cells in the habenular complex are heavily immunoreactive, as are their projection axons in the habenulo-interpeduncular tract (asterisk). The specificity of this labeling can be better appreciated by comparison with the unlabeled retrocommissural fornix (Fx) in Figure 7A. The D arrow points to dorsal, and the M arrow points to medial. **B:** Detail of the ReIn-ir neurons in the pulvinar nucleus of the thalamus (inset in A). Comparison with Figure 4I shows that, although there are a good number of immunore-

active cells, most cells in the nucleus are not labeled. **C:** Immunolabeled neurons in the lateral habenular nucleus (inset in A). **D:** ReIn-ir particles in the axons of the habenulo-interpeduncular tract. Compare with the labeling in other axonal tracts shown in Figures 1A, 2C, 3E, 6E–G. **E:** Immunoreactive neurons in the posterior nucleus. **F:** Labeling in the dorsal lateral geniculate nucleus. This image was not taken from the coronal section illustrated in A but from a more posterior a coronal section (1.6 mm caudal to the interaural plan). In F, the pial surface and the optic tract fibers (OpT) are at the top. Observe the population of heavily labeled neurons in the magnocellular layer (“C”) of the nucleus, as well as the numerous weakly labeled cells in the parvocellular layers (“A” and “A1,” which receive contra- and ipsilateral retinogeniculate inputs, respectively). For other abbreviations, see list. Scale bars = 500 μ m in A, 25 μ m in B–D, 5 μ m in E, 100 μ m in F.

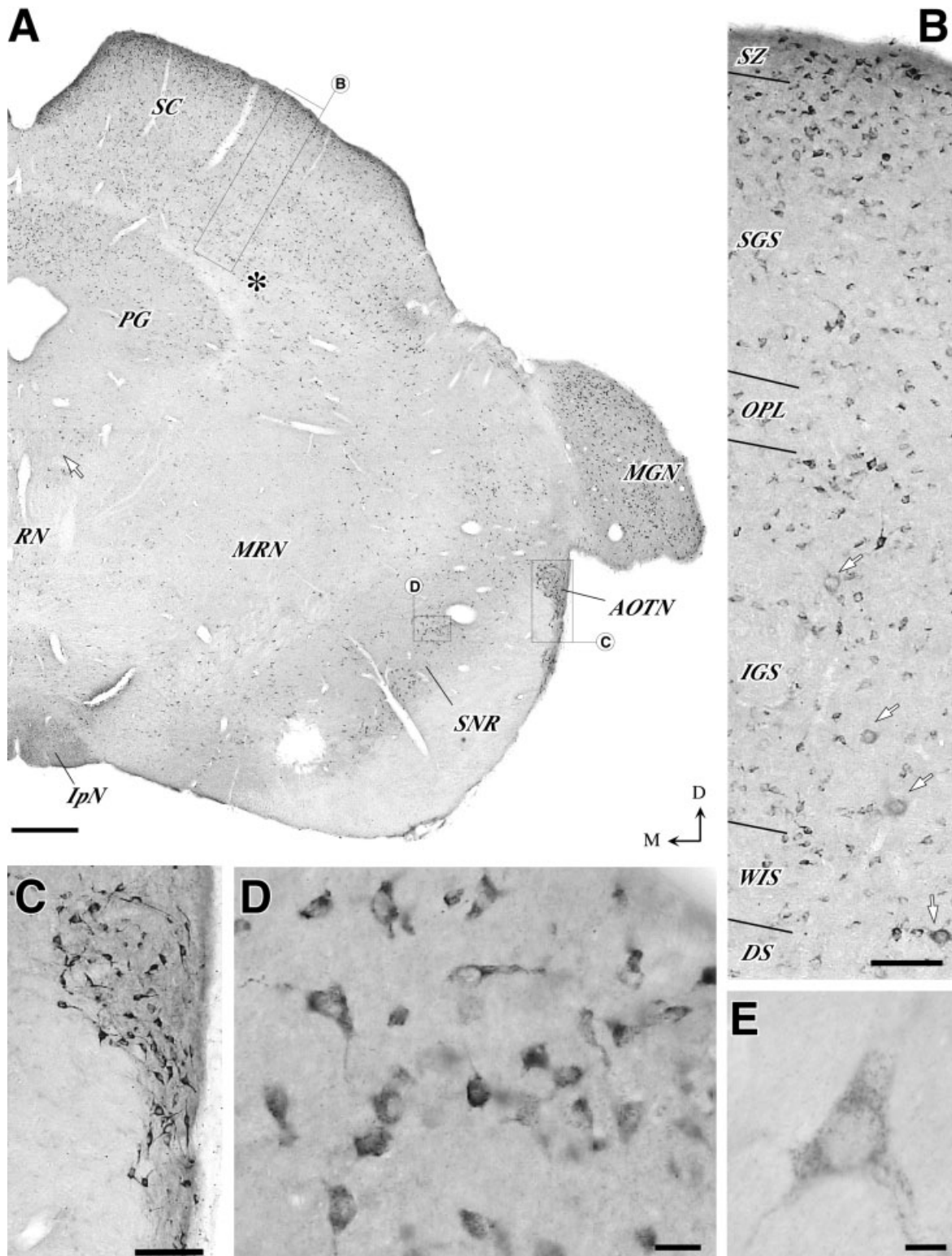


Fig. 10. Reelin-immunoreactive (ReIn-ir) neurons and neuropil in the mesencephalon. **A:** Panoramic view of the labeling in a coronal section taken 2.4 mm caudally to the interaural plane. The D arrow points to dorsal, and the “ arrow points to medial. The large numbers of neurons labeled in the medial geniculate thalamic nucleus (MGN), the superior colliculus (SC), and the accessory optic tract nuclei (AOTN) contrast with the selective labeling of fewer cell groups in the periaqueductal gray matter (PG), substantia nigra pars reticulata (SNR), and the mesencephalic reticular nucleus (MRN). Note also the heavy neuropil labeling in the superficial layer (stratum zonale) of the superior colliculus. This band exactly matches the known terminal arborization field of the retinocollicular axons. Note also the virtual absence of labeling in the oculomotor nucleus motoneurons (arrowhead). **B:** Laminar distribution of the labeling in the superior collicu-

lus. The sample corresponds to the inset in A. The pial surface is at the top. Large numbers of ReIn-ir neurons are present in all layers but particularly in the stratum zonale (SZ). In the intermediate and deep strata (IGS, WIS, DS), numerous pyramidal cells are immunolabeled (arrowheads). **C:** Detail of the labeling in AOTN (inset in A). **D:** Large multipolar immunoreactive neurons in SNR (inset in A). Note in A that the image corresponds to a cluster of ReIn-ir neurons; other portions of the nucleus are unlabeled. **E:** A large DS pyramidal cell is shown here at high magnification; its precise location is indicated by an asterisk in A. Note the particulate immunolabeling that fills the perikaryon and proximal dendrites but spares the cell nucleus. For other abbreviations, see list. Scale bars = 500 μ m in A, 100 μ m in B,C, 25 μ m in D, 10 μ m in E.

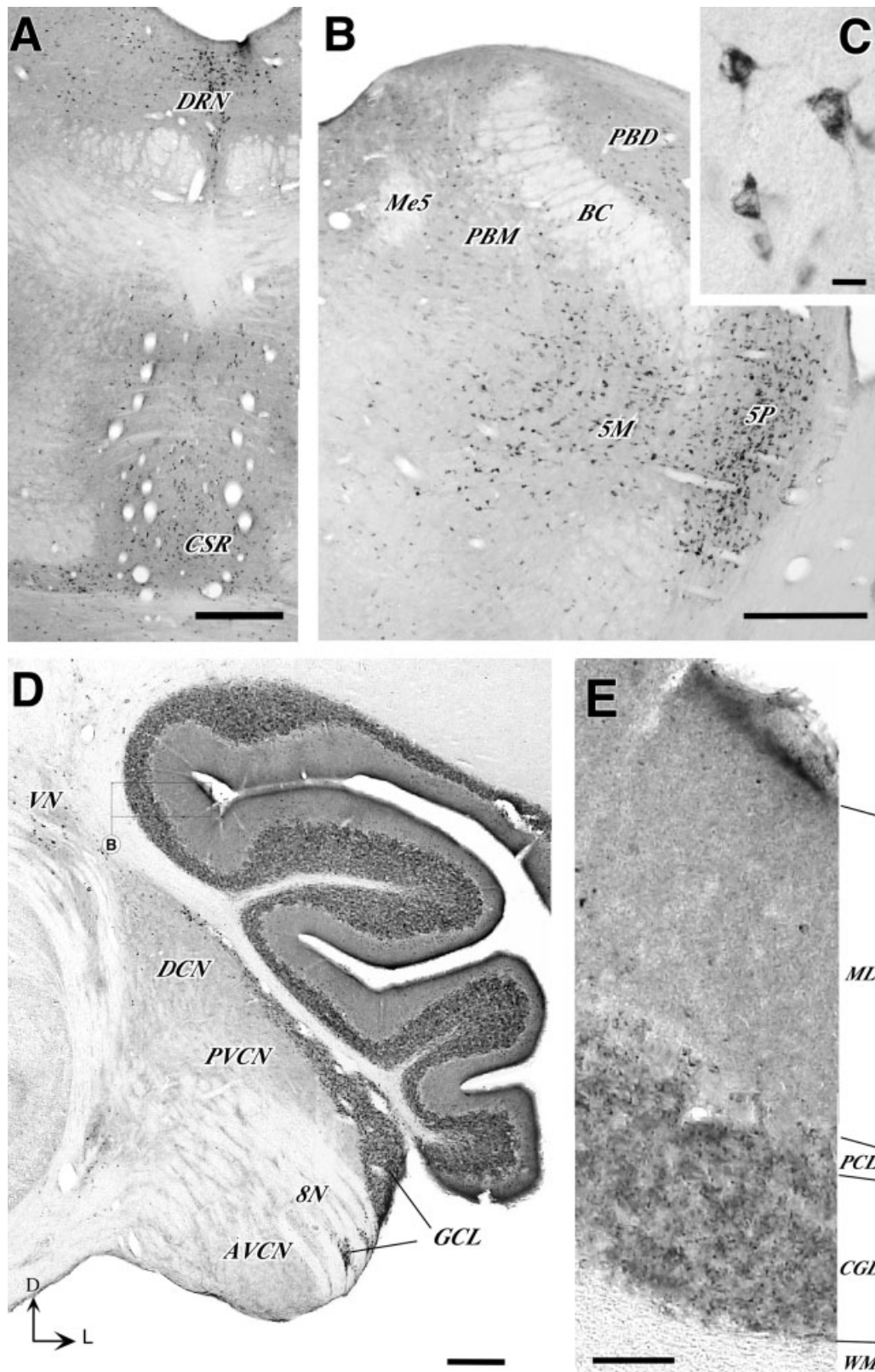


Fig. 11. Reelin-immunoreactive neurons and neuropil in the upper brainstem and cerebellum. **A:** Labeling in the raphe nuclei, midbrain tegmentum, and periaqueductal gray matter. Note the numerous heavily immunoreactive neurons in the dorsal (DRN) and central superior (CSR) raphe nuclei. **B:** Labeling in the laterodorsal quadrant of the upper pons. Large numbers of immunoreactive neurons are visible in the motor (5M) and principal trigeminal (5P) nuclei. Additional neurons are present in the dorsolateral and medial parabrachial nuclei (PBD, PBM). **C:** High-magnification view of a cells labeled in the 5M. **D:** Coronal section at the level of the entrance of the vestibulocochlear nerve (8N). A portion of the cerebellar cortex is included. Note the heavy labeling in the cerebellar cortex and in the

granule cell domains of the cochlear nuclei (GCL), whereas the remaining cochlear nuclei contain only weak neuropil labeling and no labeled somata. A few Reelin-immunoreactive neurons are present in the vestibular nuclei (VN). The D arrow points to dorsal, and the L arrow points to lateral. **E:** Laminar immunoreactivity distribution in the cerebellar cortex. Virtually all neurons in the cerebellar granule cell layer, and some occasional small neurons in the molecular layer display particulate immunolabeling in their somata. Purkinje cell somata are unlabeled. A very heavy neuropil immunolabeling expands across the entire width of the molecular layer (ML). For other abbreviations, see list. Scale bars = 500 μm in A,B, 10 μm in C, 250 μm in D, 100 μm in E.

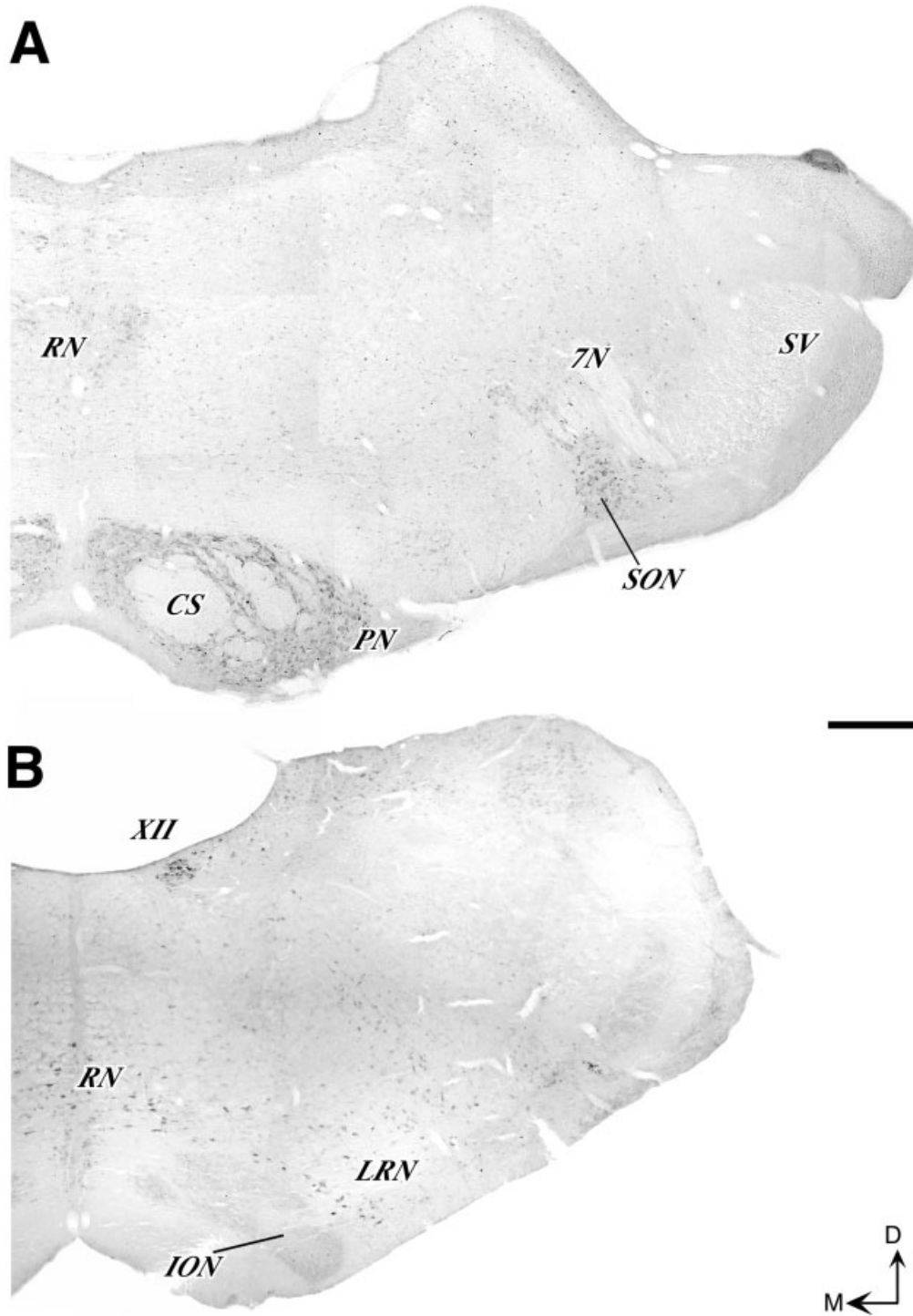


Fig. 12. Immunolabeling in the lower pons (A) and upper medulla oblongata (B). Note that, in contrast to the widespread labeling seen in forebrain and midbrain structures, Reelin-immunoreactive (ReIn-ir) neurons and neuropil at these levels are less numerous and mainly limited to specific nuclei. **A:** Coronal section taken at a caudal level of the pons. Numerous immunoreactive cells are located in the pontine nuclei (PN), the superior olivary nucleus (SON), and the

raphe nuclei (RN). Note, in addition, the neuropil labeling in the pontine nuclei. **B:** Coronal section through the upper medulla oblongata. ReIn-ir cells are mainly concentrated in the hypoglossal nucleus (XII), the raphe nuclei (RN), and the lateral reticular nucleus (LRN). Neuropil but no cells is labeled in the inferior olivary nucleus (ION). The D arrow points to dorsal, and the M arrow points to medial. For other abbreviations, see list. Scale bar = 500 μ m in A (applies to A,B).

Additional Reelin-ir somata with similar particulate perikaryal labeling were scattered in the molecular layer (Fig. 11B). Purkinje cell somata were consistently unlabeled. The entire molecular layer displayed a very heavy homogeneous neuropil labeling (Fig. 11A,B).

DISCUSSION

This is, to our knowledge, the first mapping study of Reelin in the brain of a carnivore mammal. Overall, Reelin immunoreactivity was markedly more widespread and intense in forebrain structures and the cerebellar cortex than in the brainstem, an observation coincident with recent observations in macaques (Martínez-Cerdeño et al., 2002). We have observed Reelin-immunoreactive (Reelin-ir) neuronal bodies, axonal tracts, and neuropil. The localization of these three types of immunolabeled structures is both widespread and remarkably specific. Depending on the region, the Reelin-ir neuronal somata correspond to local-circuit neurons, projection neurons, or both. The immunoreactive axonal tracts correspond to some well-defined axonal systems, such as the lateral olfactory tract, the perforant pathway, the stria terminalis, or the retroflex bundle, whereas other white matter tracts are unlabeled. A remarkable finding is that rather than solid immunolabeling, the axons in these tracts contain discrete Reelin-ir particles (Fig. 1D). Moreover, the regions known to contain the terminal arborizations of the Reelin-ir axons are also heavily immunoreactive. Taken together, these observations are consistent with the notion that neurons may anterogradely transport Reelin (Pesold et al., 1998) in membrane-bound vesicles (Derer et al., 2001) and then secrete the protein in terminal arborization fields far from their somata.

The neuronal groups that are Reelin-ir in ferrets show a basic congruence with those reported to contain Reelin protein (Miyata et al., 1996; Pesold et al., 1998; Impagnatiello et al., 1998; Guidotti et al., 2000; Rodríguez et al., 2000; Zecevic and Rakic, 2001; Pérez-García et al., 2001; Martínez-Cerdeño and Clascá, 2002; Martínez-Cerdeño et al., 2002) or mRNA (Ikeda and Terashima, 1997; Schiffman et al., 1997; Alcántara et al., 1998) in other adult mammals. At the same time, however, our findings confirm and extend the evidence for marked interspecies differences between adult mammals in the expression levels of Reelin in particular neuronal populations (Pesold et al., 1998; Martínez-Cerdeño et al., 2002; present results).

In the following discussion, we (1) compare present results in ferrets with the published data on Reelin-containing neuronal somata of the cerebral cortex and subcortical regions of other mammals, and (2) explore the implications that the axonal and neuropil immunolabeling may have for the function of Reelin in the adult mammalian brain.

Reelin-immunoreactive neuronal somata in the isocortex and hippocampus: comparison to other mammals

Reelin-immunoreactive somata in the cerebral isocortical areas of ferrets include several types of neurons in all cortical layers. As in other investigated mammal species (Miyata et al., 1996; Pesold et al., 1998; Impagnatiello et al., 1998; Guidotti et al., 2000; Rodríguez et al., 2000, 2002; Zecevic and Rakic, 2001; Pérez-García et al., 2001;

Martínez-Cerdeño and Clascá, 2002; Martínez-Cerdeño et al., 2002), the most conspicuous population of Reelin-ir neurons in the cerebral isocortex is found in layers I-II. There are, in addition, numerous other immunoreactive neurons in deeper layers (III-VI). Other interneuron types are not Reelin-ir (Pesold et al., 1998, 1999; Martínez-Cerdeño et al., 2002). The laminar distribution of Reelin-ir interneuron-like cells in the isocortex of ferrets is similar to that reported in rodents (Miyata et al., 1996; Pesold et al., 1999), whereas in macaques Reelin-ir interneurons are scant in layers V-VI (Rodríguez et al., 2000, 2002; Martínez-Cerdeño et al., 2002). As for the isocortex, the Reelin-ir interneuron populations in the hippocampal formation and entorhinal cortex of ferrets closely resemble those found in rats (Pesold et al., 1998; Drakew et al., 1998) and macaques (Martínez-Cerdeño et al., 2002). Double-labeling studies in rat and monkey cortex have shown that the cortical Reelin-ir interneurons contain γ -aminobutyric acid and belong to several morphologic types (Pesold et al., 1998, 1999; Rodríguez et al., 2000). Moreover, these studies have shown that other cortical interneurons do not contain Reelin, a finding that concurs with our observation of nonimmunoreactive neurons in layer I of the isocortex and the stratum lacunosum moleculare of the hippocampus.

In contrast to the basic similarity of the Reelin-ir cortical interneurons across species, the Reelin content of the cortical projection cells varies markedly by species. For example, in ferrets, with the exception of some faintly staining layer V neurons (Fig. 7A,B), no isocortical pyramidal cells are Reelin-ir; in rats, numerous layer V pyramidal neurons are Reelin-ir (Pesold et al., 1998; Martínez-Cerdeño and Clascá, 2002); whereas in macaques, virtually all of the isocortical pyramidal neurons are Reelin-ir (Martínez-Cerdeño and Clascá, 2002; Martínez-Cerdeño et al., 2002). Similarly, whereas the pyramidal cells of Ammon's horn and the granule cells of the dentate gyrus are Reelin-negative in ferrets (present results) and in rats (Pesold et al., 1998), they are robustly Reelin-ir in macaques (Martínez-Cerdeño et al., 2002). In the entorhinal cortex, most layer II pyramidal cells are Reelin-ir in all three mammal species; however, all layer II-V pyramidal cells are immunoreactive in macaques, whereas only some are in ferrets (in layer III), and apparently none are in rats (Pesold et al., 1998). Subcortical structures discussed below show a similar pattern of general coincidence with few consistent exceptions. Because the "incongruencies" between three evolutionarily distant mammals occur against a background of otherwise largely coincident patterns of immunolabeling with the same monoclonal antibody (no. 142; De Bergeyck et al., 1998), we believe that they reflect genuine species-specific differences in the levels of Reelin expression in some particular neuronal populations. This view is consistent with recent evidence for large quantitative differences between mammalian species in the mRNA expression and protein levels of numerous genes in equivalent brain regions (Enard et al., 2002).

Reelin immunoreactive neuronal somata in other regions: comparison to other mammals

Our data provide the first systematic report of Reelin protein distribution in the olfactory and basal forebrain

regions of an adult mammal. Results reveal that only particular neuronal populations contain Reelin, and some of them in very high amounts, whereas adjacent neuron populations are unlabeled. For example, all the mitral cells of the ferret olfactory bulb are heavily Reeln-ir, which is consistent with immunohistochemical (Pesold et al., 1998) and mRNA data in adult rodents (Schiffman et al., 1997; Alcántara et al., 1998). Remarkably, virtually none of the pyramidal cells in the adjacent anterior olfactory nucleus or in the olfactory tuberculum are Reeln-ir.

Layer II neurons of the pyriform and entorhinal cortices provide yet another striking example of the specificity of Reelin distribution in neuronal populations: the pyramidal cells superficially located in pyramidal cells in the layer are heavily Reeln-ir, whereas the deeper, apparently identical pyramidal cells are unlabeled. However, it is to be pointed out that, although the superficial part of layer II is not cytoarchitecturally distinct as a layer in carnivores, it was distinguished as a sublayer (IIa) in the rat PyC because its pyramidal neurons displayed specific dendritic morphologies and axonal connections and were somewhat more loosely packed than the deeper cells (sublayer IIb, Haberly and Price, 1978). Although equivalent data are not yet available for ferrets, given the overall similarity of the PyC in rats and ferrets, it seems likely that high Reelin content may turn out to be a consistent marker for PyC layer IIa neurons.

The distribution of Reeln-ir neuronal somata in the septum, diagonal band nuclei and substantia innominata of ferrets is comparable to that observed in equivalent nuclei of macaques. The weak but ubiquitous immunolabeling of striatal neurons is remarkably similar in both species (Martínez-Cerdeño et al., 2002; present results). In the amygdala of macaques, however, both the large projection neurons as well as the smaller interneuron-like cells are Reeln-ir, whereas in ferrets most of the larger neurons are Reelin-negative.

Large numbers of cells are immunoreactive for Reelin in the nuclei of the ferret dorsal thalamus, although the cells are relatively more abundant in some nuclei than in others (Figs. 4H,I, 8A, 9A). In most nuclei, the Reeln-ir neurons are small or medium in size, whereas the larger neurons are unlabeled. However, at least in some nuclei such as the reuniens, lateralis dorsalis, or dorsal lateral geniculate, most of the larger neurons are immunoreactive as well. Their number, shape, and distribution indicates that the Reeln-ir cells are mainly thalamic relay neurons. The relatively small size of many of them suggests that they may include the population of small and medium neurons known project to cortical layer I in carnivores (Glenn et al., 1982; Rausell and Avendaño, 1985). However, we cannot rule out the possibility that some of them are thalamic interneurons, because we did not carry out double-immunolabeling experiments combining, for example, anti-Reelin with anti- γ -aminobutyric acid or anti-glutamic acid decarboxylase antibodies. In macaques, the only other mammal species for which Reelin expression has been investigated in the adult thalamus, most relay neurons are Reeln-ir, whereas at least some of the smaller, interneuron-like thalamic cells are not Reeln-ir (Martínez-Cerdeño et al., 2002).

The reticular thalamic nucleus contains a few scattered Reeln-ir neurons in ferrets, whereas virtually all its cells are immunoreactive in macaques (Martínez-Cerdeño et

al., 2002). In contrast, the associated ventral lateral geniculate nucleus shows weak immunoreactivity for Reelin in both species.

In ferrets, the neurons in the paraventricular hypothalamic nucleus and the nucleus of the posterior commissure are prominently Reeln-ir. Remarkably, high Reelin content in equivalent cell groups has been noted in macaques (Martínez-Cerdeño et al., 2002) and rodents (Schiffman et al., 1997; Alcántara et al., 1998), and also in reptiles (Bernier et al., 1999; Goffinet et al., 1999) and birds (Bernier et al., 2000).

Reelin immunoreactivity in the pons and medulla was consistently less widespread and intense than that seen in the forebrain and mesencephalon. This preferential localization of Reelin in rostral regions of the adult central nervous system is in consonance with *in situ* hybridization studies in developing animals (Schiffman et al., 1997; Alcántara et al., 1998) as well as with the severity of the malformations in *reeler* mice (Goffinet, 1984; Phelps, 2002). Brainstem regions that contain large Reeln-ir neuronal populations in ferrets (present results) and macaques (Martínez-Cerdeño et al., 2002) include the superior and inferior colliculi, the motor and principal trigeminal, superior olivary, raphe, dorsal cochlear, pontine, and hypoglossal nuclei. Other brainstem neuronal populations are Reeln-ir in macaques but not in ferrets. Examples of this discrepancy are the mesencephalic trigeminal and the oculomotor nuclei.

As in rodents (Miyata et al., 1996; Pesold et al., 1998) and primates (Martínez-Cerdeño et al., 2002), the cerebellar cortex shows heavy immunolabeling of its granule cell layer, and of some interneurons in the molecular layer. The Purkinje cells of the cerebellar cortex are not Reeln-ir in ferrets (present results) and rodents (Miyata et al., 1996; Pesold et al., 1998), but they are strongly Reeln-ir in macaques (Martínez-Cerdeño et al., 2002).

It follows from the published reports and our own observations that, despite an evident similarity of Reelin expression patterns in equivalent neuronal populations at the various levels of the neuraxis among ferrets, macaques, and rats, there are significant differences in the levels of Reelin content for particular neuronal types (Pesold et al., 1998; Drakew et al., 1998; Rodríguez et al., 2000; Martínez-Cerdeño and Clascá 2002; Martínez-Cerdeño et al., 2002; present results). That these interspecies differences involve key neuron types such as the cortical pyramidal neurons, thalamic relay neurons, cerebellar Purkinje cells, or the brainstem motoneurons, is intriguing. Moreover, as a whole, these observations suggest a vast expansion in the extent and intensity of Reelin expression in the primate lineage.

Reelin in long axonal tracts and gray matter neuropil: functional implications

In addition to neuronal somata, our results show a widespread but selective labeling of the gray matter neuropil, as well as of some axonal tracts. This neuropil labeling consists of neurites containing bead-like particles and a homogeneous background staining. Both types of labeling were present in most gray matter regions (Table 1). Labeled neurites are likely to correspond to both terminal axonal arborizations and to dendrites, whereas the homogeneous labeling may represent the secreted, extracellular fraction of Reelin.

Our data indicate that the neurons of origin, axons, and terminal arborization fields of several axonal projection systems contain Reelin in ferrets. These Reelin-containing pathways are (1) the mitral cell projection to retrobulbar olfactory areas (anterior olfactory nucleus, pyriform cortex, olfactory tuberculum, nucleus of the lateral olfactory tract, and entorhinal cortex); (2) the entorhinohippocampal (perforant) pathway; (3) the stria terminalis; and (4) the habenulointerpeduncular pathway. These observations are consistent with the report of labeling in the lateral olfactory tract and stria terminalis axons in macaques (Martínez-Cerdeño et al., 2002). In addition, the labeling in the stratum zonale of the superior colliculus strongly suggests that a population of retinal ganglion cell axons transport and secrete Reelin in adult ferrets. Although we did not examine the retina in our ferrets, there is evidence that some retinal ganglion cells express Reelin mRNA in mice (Schiffman et al., 1997), chickens (Bernier et al., 2000), and turtles (Bernier et al., 1999).

A remarkable observation was that the axonal labeling always consisted of "rosaries" of discrete, small (0.5–1 μm) particles, whereas the rest of the axon was unlabeled (Figs. 1D, 6F,G). At low-magnification, this pattern of labeling produced a false impression of a "weak" or incomplete axon staining. At high magnification, however, the particles were found to be heavily labeled. Congruent with recent electron microscope observations in the axons of embryonic mice Cajal-Retzius cells (Derer et al., 2001), our interpretation is that these particles represent large Reelin-containing secretory vesicles that are transported anterogradely along the axons. This pattern of labeling, intriguingly reminiscent of the large neurosecretory vesicles in hypothalamohypophyseal axons (Schimchowitsch et al., 1983; Broadwell et al., 1984), suggests an abundant secretion of Reelin by some adult axonal populations.

Among the various axonal pathways found here to be richly Reelin-ir, the labeling pattern observed in the olfactory bulb projection (LOT) to olfactory areas in the basal forebrain provides compelling evidence that Reelin is transported and secreted over long distances. Comparison of our data with studies of the distribution and terminal fields of LOT axons in carnivores (Room et al., 1984) and rodents (Price, 1973; Haberly and Price, 1978) shows that the band of heavy homogeneous immunolabeling observed here matches the terminal arborization fields of LOT axons. Of interest, in some of target fields of LOT axons, such as layer I of the anterior olfactory nucleus or the olfactory tuberculum (Figs. 2, 3), the heavy homogeneous neuropil labeling is present, despite a virtual absence of Reelin neuronal somata. It follows from these observations that, at least in these fields, the heavy homogeneous Reelin immunolabeling (suggestive of secreted Reelin) is associated with terminal arborizations rather than with Reelin neuronal somata or dendrites. Moreover, the steep gradient in labeling observed between sublayers Ia and Ib suggests that secreted Reelin may reach relatively high concentrations in restricted domains near the LOT axons terminals. Our light-microscope observations indicate that a similar situation may occur in several other long projections systems, among which the perforant pathway deserves mention because of its relevance as a model for studies of synaptic plasticity. In any case, it follows from our data that anterograde axonal transport and extracellular accumulation at sites far from the synthesizing neu-

ronal somata should be factored in when addressing the *in vivo* role of Reelin in adult brain circuits.

In development, the presence of secreted functional Reelin near the pial (basal lamina) surface of the cerebral cortex has been shown to be critical for the correct positioning of migrating neuroblasts. The mechanisms for Reelin function in development involve a regulation of cell-to-cell adhesion and of cytoskeletal dynamics in both neuroblasts and glia. It is not yet fully understood whether Reelin mediates these biological effects acting as an intercellular signaling molecule, as a secreted serine-protease of the extracellular matrix, or as both (Olson and Walsh, 2002).

Remarkably, Reelin is even more widely and richly present in the adult brain than during development (Pesold et al., 1998; Drakew et al., 1998; Martínez-Cerdeño et al., 2000, 2002, present results), but there are still few clues about its function(s) in the adult. The pattern of protein localization might reveal some. For example, high levels of secreted Reelin are found in DG (Pesold et al., 1998, Martínez-Cerdeño et al., 2002; present results) where neurogenesis and subsequent migration have been shown to persist throughout adult life (Kaplan and Bell, 1984; van Praag et al., 2002). One might speculate, thus, that the presence of Reelin in the DG molecular layer could bear some relationship with the migration of newly generated granule cells (Haas et al., 2002). Nevertheless, adult neuronal migration has not been demonstrated in the other numerous cortical and subcortical regions found here to contain high amounts of Reelin.

An intriguing, and perhaps more relevant, observation is that we found the heaviest extracellular neuropil immunolabeling in precisely some of those neuropil regions (the stratum lacunosum moleculare of CA, the molecular layer of DG, PyC layer Ia, and the molecular layer of the cerebellar cortex) where rapidly inducible and long-lasting changes in synaptic efficacy have been reported to occur in the adult brain (Geinisman et al., 1992; Colbert and Levy, 1993; Klintosva and Greenough, 1999; Weeks et al., 1999; Otani et al., 1999; Vanderwolf and Zibrowski, 2001; Federmeier et al., 2002; Do et al., 2002). These plastic changes have been shown to involve large-scale rearrangements of axon terminals and dendritic spines in the adult (Geinisman et al., 1992; Klintosva and Greenough, 1999; Weeks et al., 1999; Segal, 2002). Because such cell movements occur in the complex, tightly-packed, and relatively stable neuropil of the adult brain, it is tempting to speculate that they might require some sort of specific local modulation of intercellular adhesivity and/or cytoskeletal dynamics and that extracellular Reelin may have a role in said modulation. Indeed, Reelin has been shown to be required for the normal synaptogenesis of postnatal entorhinohippocampal axons (Borrell et al., 1999). The unusually high levels of secreted Reelin in the above-mentioned neuropil regions, therefore, would be consistent with an effect of Reelin modulation of the synaptic plasticity in these circuits. This hypothesis would probably be amenable to experimental testing in the future using *in vitro* models or conditional Reelin mutants. Moreover, the presence of lower but still significant levels of Reelin in the neuropil of many other brain structures suggests that Reelin-modulated synaptic plasticity could be at play in a wide variety of adult neuronal circuits.

ACKNOWLEDGMENTS

The authors thank Dr. Alfonso Fairén for discussion, Dr. André M. Goffinet for the gift of the clone 142 antibody, Dr. Masaharu Ogawa for the CR-50 antibody, and Ms. Carol F. Warren for linguistic assistance.

LITERATURE CITED

- Alcántara S, Ruiz M, D'Arcangelo G, Ezan F, de Lecea L, Curran T, Sotelo C, Soriano E. 1998. Regional and cellular patterns of Reelin mRNA expression in the forebrain of the developing and adult mouse. *J Neurosci* 18:7779–7799.
- Avendaño C, Reinoso-Suárez F. 1975. Stereotaxic atlas of the cat's amygdala, hypothalamus and preoptic region. Madrid: Serv. Publ. Univ. Autónoma.
- Berman AL. 1968. The brain stem of the cat. A cytoarchitectonic atlas with stereotaxic coordinates. Madison: University of Wisconsin Press.
- Berman AL, Jones EG. 1982. The thalamus and basal telencephalon of the cat. A cytoarchitectonic atlas with stereotaxic coordinates. Madison: University of Wisconsin Press.
- Bernier B, Bar I, Pieau C, Lambert De Rouvroit C, Goffinet AM. 1999. Reelin mRNA expression during embryonic brain development in the turtle *Emys orbicularis*. *J Comp Neurol* 413:463–479.
- Bernier B, Bar I, D'Arcangelo G, Curran T, Goffinet AM. 2000. Reelin mRNA expression during embryonic brain development in the chick. *J Comp Neurol* 422:448–463.
- Borrell V, Del Rio JA, Alcántara S, Derer M, Martínez A, D'Arcangelo G, Nakajima K, Mikoshiba K, Derer P, Curran T, Soriano E. 1999. Reelin regulates the development and synaptogenesis of the layer-specific entorhino-hippocampal connections. *J Neurosci* 19:1345–1358.
- Broadwell RD, Cataldo AM, Balin BJ. 1984. Further studies of the secretory process in hypothalamo-neurohypophysial neurons: an analysis using immunocytochemistry, wheat germ agglutinin-peroxidase, and native peroxidase. *J Comp Neurol* 228:155–167.
- Caviness VS, Crandall JE, Edwards MA. 1988. The Reeler malformation. Implications for neocortical histogenesis. In: Peters A, Jones EG, editors. *Cerebral cortex 7*. New York: Plenum Press. p 59–89.
- Colbert CM, Levy WB. 1993. Long-term potentiation of perforant path synapses in hippocampal CA1 in vitro. *Brain Res* 606:87–91.
- D'Arcangelo G, Miao GG, Chen SC, Soares HD, Morgan JI, Curran T. 1995. A protein related to extracellular matrix proteins deleted in the mouse mutant reeler. *Nature* 374:719–723.
- D'Arcangelo G, Nakajima K, Miyata T, Ogawa M, Mikoshiba K, Curran T. 1997. Reelin is a secreted glycoprotein recognized by the CR-50 monoclonal antibody. *J Neurosci* 17:23–31.
- De Bergeyck V, Naerhuyzen B, Goffinet AM, Lambert de Rouvroit CA. 1998. Panel of monoclonal antibodies against Reelin, the extracellular matrix protein defective in reeler mutant mice. *J Neurosci Methods* 82:17–24.
- Derer P, Derer M, Goffinet A. 2001. Axonal secretion of Reelin by Cajal-Retzius cells: evidence from comparison of normal and Reln (*Orl*) mutant mice. *J Comp Neurol* 440:136–143.
- Do VH, Martínez CO, Martínez JL Jr, Derrick BE. 2002. Long-term potentiation in direct perforant path projections to the hippocampal CA3 region in vivo. *J Neurophysiol* 87:669–678.
- Drakew A, Frotscher M, Deller T, Ogawa M, Heimrich B. 1998. Developmental distribution of a reeler gene-related antigen in the rat hippocampal formation visualized by CR-50 immunohistochemistry. *Neuroscience* 82:1079–1086.
- Ekstrand JJ, Domroese ME, Feig SL, Illig KR, Haberly LB. 2001. Immunocytochemical analysis of basket cells in rat piriform cortex. *J Comp Neurol* 434:308–328.
- Enard W, Khaitovich P, Klose J, Zöllner S, Heissig F, Giavalisco P, Nieselt-Struwe K, Muchmore E, Varki A, Ravid R, Doxiadis GM, Bontrop RE, Pääbo S. 2002. Intra- and interspecific variation in primate gene expression patterns. *Science* 296:340–343.
- Falconer DS. 1951. Two new mutants, 'trembler' and 'reeler' with neurological action in the house mouse (*Mus musculus L.*) *J Genet* 50:192–201.
- Federmeier KD, Kleim JA, Greenough WT. 2002. Learning-induced multiple synapse formation in rat cerebellar cortex. *Neurosci Lett* 332:180–184.
- Geinisman Y, de Toledo-Morrell L, Morrell F, Persina IS, Rossi M. 1992. Structural synaptic plasticity associated with the induction of long-term potentiation is preserved in the dentate gyrus of aged rats. *Hippocampus* 2:445–456.
- Glenn LL, Hada J, Roy JP, Deschenes M, Steriade M. 1982. Anterograde tracer and field potential analysis of the neocortical layer I projection from nucleus ventralis medialis of the thalamus in cat. *Neuroscience* 7:1861–1877.
- Goffinet AM. 1984. Events governing organization of postmigratory neurons: studies on brain development in normal and reeler mice. *Brain Res* 319:261–296.
- Goffinet AM, Bar I, Bernier B, Trujillo C, Raynaud A, Meyer G. 1999. Reelin expression during embryonic brain development in lacertilian lizards. *J Comp Neurol* 414:533–550.
- Guidotti A, Auta J, Davis JM, Gerevini VD, Dwivedi Y, Grayson DR, Impagnatiello F, Pandey G, Pesold C, Sharma R, Uzunov D, Costa E. 2000. Decrease in Reelin and glutamic acid decarboxylase 67 (GAD67) expression in schizophrenia and bipolar disorder: a postmortem brain study. *Arch Gen Psychiatry* 57:1061–1069.
- Haas CA, Dudeck O, Kisch M, Huzsaka C, Kann G, Pollack S, Zentner J, Frotscher M. 2002. Role for reelin in the development of granule cell dispersion in temporal lobe epilepsy. *J Neurosci* 22:5797–5802.
- Haberly LB, Price JL. 1978. Association and commissural fiber systems of the olfactory cortex of the rat. *J Comp Neurol* 178:711–740.
- Heymann R, Kallenbach S, Alonso S, Carroll P, Mitsiadis TA. 2001. Dynamic expression patterns of the new protocadherin families CNRs and Pcdh-gamma during mouse odontogenesis: comparison with Reelin expression. *Mech Dev* 106:181–184.
- Hong SE, Shugart YY, Huang DT, Shahwan SA, Grant PE, Hourihane JO, Martin ND, Walsh CA. 2000. Autosomal recessive lissencephaly with cerebellar hypoplasia is associated with human RELN mutations. *Nat Genet* 26:93–96.
- Ikeda Y, Terashima T. 1997. Expression of Reelin, the gene responsible for the reeler mutation, in embryonic development and adulthood in the mouse. *Dev Dyn* 210:157–72.
- Impagnatiello F, Guidotti AR, Pesold C, Dwivedi Y, Caruncho H, Pisu MG, Uzunov DP, Smalheiser NR, Davis JM, Pandey GN, Pappas GD, Tueting P, Sharma RP, Costa E. 1998. A decrease of Reelin expression as a putative vulnerability factor in schizophrenia. *Proc Natl Acad Sci U S A* 95:15718–15723.
- Jossin Y, Goffinet AM. 2001. Reelin does not directly influence axonal growth. *J Neurosci* 21:RC183.
- Kaplan MS, Bell DH. 1984. Mitotic neuroblasts in the 9-day-old and 11-month-old rodent hippocampus. *J Neurosci* 4:1429–1441.
- Klintsova AY, Greenough WT. 1999. Synaptic plasticity in cortical systems. *Curr Opin Neurobiol* 9:203–208.
- Krettek JE, Price JL. 1977. Projections from the amygdaloid complex and adjacent structures to the cerebral cortex and thalamus in the cat and rat. *J Comp Neurol* 172:687–722.
- Lacor PN, Grayson DR, Auta J, Sugaya I, Costa E, Guidotti A. 2000. Reelin secretion from glutamatergic neurons in culture is independent from neurotransmitter regulation. *Proc Natl Acad Sci U S A* 97:3556–3561.
- Linden DC, Guillery RW, Cucchiari J. 1981. The dorsal lateral geniculate nucleus of the normal ferret and its postnatal development. *J Comp Neurol* 203:189–211.
- Martínez-Cerdeño V, Clascá F. 2002. Reelin immunoreactivity in the adult neocortex: a comparative study in rodents, carnivores and non-human primates. *Brain Res Bull* 57:485–488.
- Martínez-Cerdeño V, Galazo MJ, Fairén A, Clascá F. 2000. Reelin immunoreactivity in the cerebral cortex of embryonic and postnatal ferrets. *Eur J Neurosci* 12 S11:327.
- Martínez-Cerdeño V, Galazo MJ, Cavada C, Clascá F. 2002. Reelin immunoreactivity in the adult primate brain: intracellular localization in projecting and local circuit neurons of the cerebral cortex, hippocampus, and subcortical regions. *Cereb Cortex* 12:1298–1311.
- Miyata T, Nakajima K, Aruga J, Takahashi S, Ikenaka K, Mikoshiba K, Ogawa M. 1996. Distribution of a reeler gene-related antigen in a developing cerebellum: an immunohistochemical study with an allo-genic antibody CR-50 in normal and reeler mice. *J Comp Neurol* 372:215–228.
- Noctor SC, Palmer SL, Hasling T, Juliano SL. 1999. Interference with the development of early generated neocortex results in disruption of radial glia and abnormal formation of neocortical layers. *Cereb Cortex* 9:121–136.
- Olson Y, Walsh CA. 2002. Smooth, rough and upside-down neocortical development. *Curr Opin Genet Dev* 12:320–327.

- Otani S, Auclair N, Desce JM, Roisin MP, Crepel F. 1999. Dopamine receptors and groups I and II mGluRs cooperate for long-term depression induction in rat prefrontal cortex through converging postsynaptic activation of MAP kinases *J Neurosci* 19:9788–9802.
- Pappas GD, Kriho V, Pesold C. 2002. Reelin in the extracellular matrix and dendritic spines of the cortex and hippocampus: a comparison between wild type and heterozygous reeler mice by immunoelectron microscopy. *J Neurocytol* 20:413–425.
- Pérez-García CG, Gonzalez-Delgado FJ, Suarez-Sola ML, Castro-Fuentes R, Martín-Trujillo JM, Ferrer-Torres R, Meyer G. 2001. Reelin-immunoreactive neurons in the adult vertebrate pallium. *J Chem Neuroanat* 21:41–51.
- Pesold C, Liu WS, Guidotti A, Costa E, Caruncho HJ. 1999. Cortical bitufted, horizontal, and Martinotti cells preferentially express and secrete Reelin into perineuronal nets, nonsynaptically modulating gene expression. *Proc Natl Acad Sci U S A* 96:3217–3222.
- Pesold C, Pisu M, Impagnatiello F, Uzunov DP, Caruncho HJ. 1998. Simultaneous detection of glutamic acid decarboxylase and Reelin mRNA in adult rat neurons using in situ hybridization and immunofluorescence. *Brain Res Brain Res Protoc* 3:155–160.
- Phelps PE, Rich R, Dupuy-Davies S, Ríos Y, Wong T. 2002. Evidence for a cell-specific action of Reelin in the spinal cord. *Dev Biol* 244:180–198.
- Price JL. 1973. An autoradiographic study of complementary laminar patterns of termination of afferent fibers to the olfactory cortex. *J Comp Neurol* 150:87–108.
- Quattrocchi CC, Wannenes F, Persico AM, Ciafre SA, D'Arcangelo G, Farace MG, Keller F. 2002. Reelin is a serine protease of the extracellular matrix. *J Biol Chem* 277:303–309.
- Rausell E, Avendaño C. 1985. Thalamocortical neurons projecting to superficial and to deep layers in parietal, frontal and prefrontal regions in the cat. *Brain Res* 347:159–165.
- Rice DS, Curran T. 2001. Role of the Reelin signaling pathway in central nervous system development. *Annu Rev Neurosci* 24:1005–1039.
- Rodríguez MA, Pesold C, Liu WS, Kriho V, Guidotti A, Pappas GD, Costa E. 2000. Colocalization of integrin receptors and Reelin in dendritic spine postsynaptic densities of adult nonhuman primate cortex. *Proc Natl Acad Sci U S A* 97:3550–3555.
- Rodríguez MA, Caruncho HJ, Costa E, Pesold C, Liu W-S, Guidotti A. 2002. *J Comp Neurol* 451:279–288.
- Room P, Groenewegen HJ. 1986. Connections of the parahippocampal cortex in the cat. I. Cortical afferents. *J Comp Neurol* 251:415–450.
- Room P, Groenewegen HJ, Lohman AHM. 1984. Inputs from the olfactory bulb and olfactory cortex to the entorhinal cortex in the cat. *Exp Brain Res* 56:488–496.
- Schiffmann SN, Bernier B, Goffinet AM. 1997. Reelin mRNA expression during mouse brain development. *Eur J Neurosci* 9:1055–1071.
- Schimchowitz S, Stoeckel ME, Klein MJ, Garaud JC, Schmitt G, Porte A. 1983. Oxytocin-immunoreactive nerve fibers in the pars intermedia of the pituitary in the rabbit and hare. *Cell Tissue Res* 228:255–263.
- Segal M. 2002. Changing views of Cajal's neuron: the case of the dendritic spine. *Prog Brain Res* 136:101–107.
- Smalheiser NR, Costa E, Guidotti A, Impagnatiello F, Auta J, Lacor P, Kriho V, Pappas GD. 2000. Expression of Reelin in adult mammalian blood, liver, pituitary pars intermedia, and adrenal chromaffin cells. *Proc Natl Acad Sci U S A* 97:1281–1286.
- van Praag H, Schinder AF, Christie BR, Toni N, Palmer TD, Gage FH. 2002. Functional neurogenesis in the adult hippocampus. *Nature* 415:1030–1034.
- Vanderwolf CH, Zibrowski EM. 2001. Pyriform cortex beta-waves: odor-specific sensitization following repeated olfactory stimulation. *Brain Res* 892:301–308.
- Weeks AC, Ivancic TL, Leboutillier JC, Racine RJ, Petit TL. 1999. Sequential changes in the synaptic structural profile following long-term potentiation in the rat dentate gyrus: I. The intermediate maintenance phase. *Synapse* 31:97–107.
- Witter MP, Groenewegen HJ. 1984. Laminar origin and septotemporal distribution of entorhinal and perirhinal projections to the hippocampus in the cat. *J Comp Neurol* 224:371–385.
- Zecevic N, Rakic P. 2001. Development of layer I neurons in the primate cerebral cortex. *J Neurosci* 21:5607–5619.
- Zhang HY, Hoffmann KP. 1993. Retinal projections to the pretectum, accessory optic system and superior colliculus in pigmented and albino ferrets. *Eur J Neurosci* 5:486–500.